sustainability

Article

Advancing Shear Capacity Estimation in Rectangular RC Beams: A Cutting-Edge Artificial Intelligence Approach for Assessing the Contribution of FRP

Nima Ezami [1,2], Aybike Özyüksel Çiftçioğlu [3], Masoomeh Mirrashid [4] and Hosein Naderpour [4,5,*]

1 Department of Civil and Mineral Engineering, University of Toronto, Toronto, ON M5S 1A4, Canada
2 GEI Consultants Inc., Markham, ON L3R 4M8, Canada
3 Department of Civil Engineering, Faculty of Engineering, Manisa Celal Bayar University, Manisa 45140, Turkey
4 Faculty of Civil Engineering, Semnan University, Semnan 35131-19111, Iran
5 Department of Civil Engineering, Toronto Metropolitan University, Toronto, ON M5B 2K3, Canada
* Correspondence: hosein.naderpour@torontomu.ca or naderpour@semnan.ac.ir

Abstract: Shear strength prediction in FRP-bonded reinforced concrete beams is crucial for ensuring structural integrity and safety. In this extensive investigation, advanced machine learning algorithms are harnessed to achieve precise shear strength predictions for rectangular RC beams reinforced with FRP sheets. The aim of this research is to enhance the accuracy and reliability of shear strength estimation, providing valuable insights for the design and assessment of FRP-strengthened structures. The primary contributions of this study lie in the meticulous comparison of various machine learning algorithms, including Xgboost, Gradient Boosting, Random Forest, AdaBoost, K-nearest neighbors, and ElasticNet. Through comprehensive evaluation based on predictive performance, the most suitable model for accurately estimating the shear strength of FRP-reinforced rectangular RC beams is identified. Notably, Xgboost emerges as the superior performer, boasting an impressive R^2 value of 0.901. It outperforms other algorithms and demonstrates the lowest RMSE, MAE, and MAPE values, establishing itself as the most accurate and reliable predictor. Furthermore, a sensitivity analysis is conducted using artificial neural networks to assess the influence of input variables. This additional research facet sheds light on the critical factors shaping shear strength outcomes. The study, as a whole, represents a substantial contribution to advancing the development of accurate and dependable prediction models. The practical implications of this work are far-reaching, particularly for engineering applications in the realm of structures reinforced with FRP. The findings have the potential to transform the approach to the design and assessment of such structures, elevating safety, efficiency, and performance to new heights.

Keywords: capacity; FRP; rectangular RC beams; estimation; artificial intelligence

check for updates

Citation: Ezami, N.; Özyüksel Çiftçioğlu, A.; Mirrashid, M.; Naderpour, H. Advancing Shear Capacity Estimation in Rectangular RC Beams: A Cutting-Edge Artificial Intelligence Approach for Assessing the Contribution of FRP. *Sustainability* **2023**, *15*, 16126. https://doi.org/10.3390/su152216126

Academic Editor: Ramadhansyah Putra Jaya

Received: 23 September 2023
Revised: 7 November 2023
Accepted: 16 November 2023
Published: 20 November 2023

Copyright: © 2023 by the authors. Licensee MDPI, Basel, Switzerland. This article is an open access article distributed under the terms and conditions of the Creative Commons Attribution (CC BY) license (https://creativecommons.org/licenses/by/4.0/).

1. Introduction

Concrete structures are extensively employed in the construction industry due to their high strength and durability. [1]. However, they often experience shear failures, which can lead to catastrophic consequences. In the pursuit of enhancing the shear strength of concrete beams, many methods have been developed, among which the external bonding of FRP composites has emerged as a subject of substantial research and scholarly focus [2]. The use of FRP composites as an external bonding technique has shown great promise in enhancing the structural performance of concrete elements, mitigating shear failures, and increasing their load-carrying capacity [3]. The extant literature exhibits a plethora of scholarly endeavors exploring the domain of shear strengthening of concrete beams through the utilization of FRP sheets. This compendium of studies exemplifies the substantial research endeavors and notable progress achieved within this realm. Encompassing a diverse array of subjects, these investigations span experimental inquiries, analytical modeling approaches, numerical simulations, and the development of design guidelines.

De Maio et al. [4] evaluated the impact of damage on the dynamic characteristics of RC structures retrofitted with FRP systems. A numerical model, utilizing a cohesive crack strategy and an embedded truss model, was performed to simulate the damage progression under quasi-static loading conditions. The dynamic response, specifically the natural vibration frequencies, was analyzed and compared to numerical and experimental results. The findings demonstrate that the FRP system positively influences both the static and dynamic behavior of the structures, enhancing their load-carrying capacity and mitigating natural frequency degradation. A comprehensive literature review on the utilization of natural fibers and biopolymers in FRP composites for concrete members was presented by Nwankwo et al. [5]. The study examines various FRP configurations and strengthening techniques, placing emphasis on the effectiveness of bio-based FRPs in enhancing the strength of concrete beams and columns. The review emphasizes the importance of factors such as laminate thickness, FRP anchorage, and member stiffness in determining the effectiveness of the strengthening process. Furthermore, analytical and numerical modeling methods are identified as valuable tools for predicting the behavior of concrete structures bonded with bio-based FRPs. The authors also acknowledge the impact of environmental factors on bio-based FRPs and discuss the potential for modifying natural fiber properties through appropriate treatments. Zhou et al. [6] presented a comprehensive review of stochastic multiscale analysis for FRP composite structures. The research focuses on the uncertainties in FRP structures that are caused by material variations and manufacturing processes. Key aspects discussed include the source of uncertainty, the prediction of effective material properties with uncertainties, and probabilistic structural analysis. Manufacturing weaknesses like fiber misalignment and matrix voids have a significant influence on the mechanical properties of FRP composites. Techniques based on micromechanics and probabilistic homogenization are employed to predict and quantify the impact of microscale uncertainties on overall material behavior. The integration of probabilistic homogenization and structural analysis enables multi-scale stochastic analysis, providing more accurate results than single-scale approaches. The review emphasizes the need for further research to consider realistic uncertainties, propagate non-probabilistic random variables across scales, and explore nonlinear problems and non-probabilistic reliability analysis.

Zhang et al. [7] investigated flexural design in RC structures strengthened by hybrid bonded-FRP. Their study addresses the lack of effective design methodologies for this strengthening technique. The authors analyze debonding mechanisms and failure modes, propose a design process, and introduce failure criteria that ensure good ductility. They develop a predictive model for bearing capacity and verify its accuracy. Numerical analysis confirms the effectiveness of the fastener design. Pohoryles et al. [8] studied the impact of slabs and transverse beams on the effectiveness of FRP retrofitting for existing RC structures under seismic loading. Through experimental investigations conducted on four beam-column joints, they revealed that the presence of slabs and transverse beams significantly influences damage progression and failure mechanisms. The retrofit effectiveness is found to be higher in specimens without slabs and transverse beams, indicating the inadequacy of focusing solely on joint shear strengthening. These findings caution against overestimating the effectiveness of retrofitting and emphasize the importance of accurately representing realistic structures in numerical and experimental assessments for assessing seismic performance in RC moment-resisting frames. In another research work, Wei et al. [9] conducted experiments to investigate the dynamic properties of eight footbridges constructed using FRP composites. They compare these properties to six additional FRP footbridges as well as 124 non-FRP footbridges. The comprehensive analysis reveals that FRP footbridges exhibit similar basic frequencies but higher damping ratios compared to conventional materials. The natural frequencies and damping ratios of FRP footbridges are found to be response amplitude dependent. The presence of accelerant peaks suggests that FRP footbridges exhibit approximately 3.5 times higher responsiveness to resonant excitation compared to conventional bridges of similar length and mode shape.

Ferracuti [10] proposed a model for retrofitting RC frames using FRP wrapping specifically for columns subjected to axial loading and cyclic bending, which is a common scenario in seismic areas. The present models for FRP-bonded RC frames primarily consider pure axial loads, neglecting the effects of cyclic bending. The proposed model takes into account the strain gradient effect caused by bending loads, which significantly affects the confinement level of the frame. The validation of the model was established through a comprehensive comparison of its results with the experimental data obtained from cyclic tests. Additionally, the model is incorporated into open-source software, enabling its utilization for conducting pushover analyses on an existing RC frame. This analysis investigates various retrofitting strategies aimed at improving column ductility in response to lateral forces. A novel numerical method for seismic assessment of RC structures, considering both bare and FRP-retrofitted conditions was proposed by Markou et al. [11]. The method incorporates a damage factor in the steel constitutive material model, which accurately represents the accumulated damage in the surrounding concrete and accounts for bar slippage. Experimental validation is performed using full-scale cyclic tests on deficient RC joints wrapped with CFRP, showing good agreement between the proposed model and observed nonlinear behavior. The results highlight the method's robustness and accuracy in capturing extreme nonlinearities, providing a basis for reliable numerical tools and design guidelines for seismic evaluation of structures pre- and post-earthquake events. Furthermore, Ding et al. [12] introduced a novel vibration-based approach for detecting debonding in FRP-strengthened structures using an evolutionary model. The study addresses the limitations of conventional nondestructive testing methods by proposing a global vibration-based method that can identify debonding conditions even at locations far from the sensors. Experimental tests on an FRP-strengthened cantilever steel beam were conducted, simulating debonding scenarios through a stepwise bonding procedure. By extracting natural frequencies and mode shapes and employing model updating with l0.5 regularization, the proposed algorithm accurately locates and quantifies the debonding condition. The integration of K-means clustering in the Q-learning approach enhances the optimization process.

Zeng et al. [13] presented the development and flexural behavior of FRP bar-reinforced ultra-high-performance concrete (UHPC) plates with a grouting sleeve connection. By incorporating FRP bars and steel grouting sleeves, the innovative connection method offers a dependable solution for the prefabrication construction of UHPC structures reinforced with FRP bars. Through comprehensive flexural tests, the impact of the connection mode and the type of reinforcing fiber embedded in the UHPC is thoroughly examined. The findings demonstrate that the proposed system ensures reliable performance, as failure occurs outside the connection zone. Also, Wu et al. [14] introduced a novel approach for modeling and predicting the mechanical behavior of FRP-wrapped slabs through the development of two multilayer composite plates. These elements integrate the substrate, and FRP sheet into a single element, effectively addressing the challenges associated with geometric irregularities and time-varying adhesive properties. By offering the capability to simulate irregular structures and achieve enhanced accuracy, these elements enable the accurate analysis of various strengthening systems.

In light of the potential catastrophic consequences associated with shear failures in concrete structures, there is an urgent need to explore innovative approaches that can enhance their shear strength. Among the promising research avenues, the implementation of machine learning (ML) models arises as a compelling solution [15–17]. These models have the potential to provide invaluable insights into the intricate behavior of FRP-strengthened RC beams by leveraging the power of data-driven analysis.

This study addresses a significant research gap in the body of knowledge by improving our understanding of and ability to predict the shear strength of concrete beams wrapped with FRP. Shear failures in concrete structures can have detrimental effects, such as structural harm or safety risks. This study aims to provide engineers with reliable tools for evaluating the shear strength performance of FRP-strengthened RC beams by investigating novel approaches and utilizing the power of ML models.

The use of FRP composites as an external bonding technique has shown great promise in improving the structural performance of concrete members, mitigating shear failures, and increasing their load-carrying capacity. However, accurately predicting the shear strength of FRP-strengthened concrete beams is a complicated task due to the intricate interplay between various wrapping techniques and fiber types.

The application of FRP in enhancing the shear capacity of reinforced concrete beams offers a pathway to mitigate reliance on conventional materials like steel, known for its substantial environmental footprint. Optimizing existing structures with innovative materials such as FRP advocates for sustainable resource utilization and a reduction in carbon emissions. The focus on Durability extends beyond lessening environmental impact to encompass the longevity of structures. Emphasizing the bolstering of the shear capacity of RC beams correlates with the potential for prolonged infrastructure lifespan. This extension diminishes the necessity for frequent repairs and reconstructions, practices known for their resource-intensive and environmentally adverse consequences. Furthermore, the research addresses Waste Reduction, a crucial aspect of sustainable building practices. Introducing FRP for retrofitting existing structures holds promise in minimizing the demolition and disposal of outdated constructions. This strategy adheres to sustainability principles by curbing construction-related waste and mitigating associated environmental repercussions. Moreover, the study contributes to Energy Efficiency, a pivotal element in sustainable construction. Retrofitting RC beams with FRP enhances building performance, making structures more resilient to natural disasters and adverse conditions. This fortification diminishes the energy consumption and resources typically required for reconstruction.

2. Materials and Methods

This study aims to examine the effectiveness of ML models in predicting the shear strength of concrete beams externally bonded with FRP. The analysis includes a comprehensive database containing various types of wrapping techniques and fiber types commonly used in FRP strengthening applications. The database includes three types of wrapping techniques: U-wrap (U), side bonded (SB), and closed wrap (F). Each of these techniques provides a distinct method of applying FRP composites to concrete beams, thereby influencing their shear behavior. Furthermore, the database includes four types of fibers: carbon fiber-reinforced polymer (CFRP), basalt fiber-reinforced polymer (BFRP), glass fiber-reinforced polymer (GFRP), and polyethylene terephthalate fiber-reinforced polymer (PET-FRP). These fiber types have varying mechanical properties, which adds to the variability in shear performance of FRP-strengthened concrete beams.

The comprehensive database used in this study, which includes various wrapping techniques and fiber types, allows for an in-depth analysis of the factors influencing shear behavior, as presented in Appendix A. In pursuit of accomplishing the objective of shear strength prediction, we employ a range of ML models, each incorporating state-of-the-art methodologies. These models include eXtreme Gradient Boosting (Xgboost), Random Forest (RF), Adaptive Boosting (Adaboost), ElasticNet, K-nearest neighbors (KNN), and Gradient Boosting (GB). Using these models, we aim to develop accurate and reliable prediction frameworks that will aid engineers in assessing the shear strength of FRP-strengthened RC beams. The ML models were implemented using Python 3.7. The following Python libraries were used: NumPy, SciPy, Pandas, Matplotlib, and TensorFlow. The study aims to provide engineers with reliable tools that will help in the design and evaluation of FRP-strengthened beams, thereby improving the safety and performance of structures.

The significance of this study extends across multiple dimensions. Firstly, it addresses the critical issue of mitigating the risks associated with shear failures in concrete structures, thereby contributing to overall structural safety. Secondly, the use of ML models provides a robust and efficient solution for predicting shear strength, outperforming traditional methods and providing more precise and reliable assessments. This advancement has the potential to revolutionize the field of FRP strengthening, empowering engineers to make informed decisions regarding the design and performance evaluation of FRP-strengthened RC beams. Additionally, the comprehensive database employed in this research enhances the applicability and generalizability of the developed prediction frameworks, making them relevant to a wide range of practical scenarios. Overall, this study significantly contributes to advancing the understanding and implementation of FRP strengthening techniques, thereby promoting the development of resilient and sustainable concrete structures.

2.1. Extreme Gradient Boosting

XGBoost is a powerful ensemble learning algorithm that has gained widespread popularity in ML and data science applications. It belongs to the family of gradient-boosting algorithms, which are known for their high predictive accuracy and robustness in handling a variety of data types and complexities. XGBoost stands out for its efficiency and effectiveness in handling structured data, as well as its ability to handle missing values, making it a versatile tool for a wide range of applications, including classification, regression, ranking, and even more complex tasks like user-defined custom objectives. The algorithm is built on the principles of boosting, which involves combining the predictions of multiple weak learners (typically decision trees) to create a strong learner. It sequentially builds a series of trees, each attempting to correct the errors of the previous ones. This iterative process allows XGBoost to continually refine its predictions, resulting in a highly accurate model [18].

The advantages of the Xgboost algorithm can be summarized as follows:

1. High Predictive Accuracy: XGBoost often outperforms other ML algorithms in terms of predictive accuracy. It effectively reduces bias and variance, leading to models that generalize well to new, unseen data.
2. Efficiency and Scalability: XGBoost is engineered for efficiency and speed. It employs a number of optimization techniques, including parallelization and approximation algorithms, which make it highly scalable and capable of handling large datasets.
3. Feature Importance: XGBoost provides a feature importance score, allowing users to understand which features have the most impact on the model's predictions. This information is crucial for feature selection and understanding the underlying relationships in the data.
4. Robustness to Overfitting: The algorithm includes regularization terms, such as L1 (Lasso) and L2 (Ridge) penalties, which help prevent overfitting. This ensures that the model does not become overly complex and remains capable of generalizing to unseen data.
5. Handling Missing Values: XGBoost has a built-in mechanism to handle missing values during the training process, reducing the need for extensive data preprocessing.

The disadvantages of the Xgboost algorithm can be summarized as follows:

1. Black-Box Nature: Like many ensemble methods, the interpretability of XGBoost models can be a challenge. Understanding the exact decision-making process within the model can be complex, especially when dealing with a large number of features and trees.
2. Resource Intensive: Although XGBoost is efficient, it can be computationally demanding, especially when training very large models on limited hardware. This may limit its practicality in resource-constrained environments.
3. Sensitivity to Hyperparameters: The proper tuning of hyperparameters is crucial for achieving optimal performance with XGBoost. This process can be time-consuming and may require some expertise.
4. Limited Support for Unstructured Data: XGBoost is designed primarily for structured data. It may not perform as effectively when applied to unstructured data types, such as text, images, or audio, without appropriate feature engineering.

5. Potential for Overfitting: While XGBoost is designed to mitigate overfitting, it is not immune to it. Improper hyperparameter tuning or the use of very complex models can still lead to overfitting issues. Regularization techniques must be applied judiciously.

In summary, XGBoost is a highly effective algorithm known for its predictive accuracy, efficiency, and robustness. However, it may require careful tuning and may not be the best choice for all types of data or applications. Researchers and practitioners should consider its advantages and disadvantages in the context of their specific use case.

2.2. Random Forest

RF is an ensemble learning method that is used in both classification and regression tasks [19]. It operates by constructing multiple decision trees during the training phase and outputs the class (in classification tasks) or mean prediction (in regression tasks) of the individual trees. During the training process, RF randomly selects a subset of features and a subset of the training data for each tree, which helps in reducing overfitting. It then builds multiple decision trees based on these subsets. In the case of classification, each tree 'votes' for a class, and the class with the most votes is considered the final prediction. For regression, the predictions of the individual trees are averaged to obtain the final output.

The advantages of the RF algorithm can be summarized as follows:

1. High Predictive Accuracy: RF is renowned for its remarkable predictive accuracy. Combining the predictions of multiple decision trees effectively reduces overfitting, providing more reliable and accurate results compared to single decision trees.
2. Robustness to Outliers: RF is robust against outliers and noisy data, as individual decision trees can be sensitive to extreme values. The ensemble nature of RF mitigates the impact of such anomalies on the overall model.
3. Feature Importance: RF can evaluate the importance of features in the dataset. It assigns a relevance score to each feature, aiding in feature selection and providing insights into which attributes contribute most to the model's predictions.
4. Handling Missing Data: It can handle missing data without extensive data preprocessing. Using surrogate splits, RF can make predictions based on available information, making it more resilient to incomplete datasets.
5. Reduction in Overfitting: RF reduces the risk of overfitting, a common problem in decision trees, by introducing randomness through feature subsampling and bootstrapping. This helps the model to generalize better to unseen data.
6. Parallelization: RF can efficiently utilize parallel processing, as individual trees can be constructed independently. This makes it suitable for large datasets and computationally intensive tasks.
7. Interpretability: While not as interpretable as a single decision tree, RF can provide insights into feature importance and how the model makes predictions, aiding in model understanding and feature engineering.

The disadvantages of the RF algorithm can be summarized as follows:

1. Complexity: The ensemble of multiple decision trees can make the RF model complex, potentially requiring more memory and computational resources compared to single-decision trees.
2. Computational Cost: Training an RF model can be computationally expensive, especially for large datasets or a high number of trees in the forest.
3. Black-Box Nature: RFs are less interpretable compared to individual decision trees, making it challenging to understand the inner workings of the model, especially when dealing with a large number of trees.
4. Not Suitable for Linear Relationships: RF may not perform as well as linear models when the underlying relationship between features and the target variable is linear, as it is inherently a non-linear model.

5. Overhead in Hyperparameter Tuning: Tuning the hyperparameters of an RF, such as the number of trees and the depth of the tree, can be time-consuming and require careful experimentation to achieve optimal performance.

In conclusion, RF is a powerful and versatile ensemble learning method with several advantages, including high predictive accuracy, robustness, and feature importance analysis. However, it also has its disadvantages, such as complexity, computational cost, and reduced interpretability, which should be considered when choosing this method for a specific ML task.

2.3. AdaBoost

AdaBoost is an ensemble learning method used in classification and regression tasks [20]. It works by combining the predictions of multiple weak learners (typically decision trees) to form a strong learner. The key idea behind AdaBoost is to sequentially train a series of weak models, giving more weight to misclassified samples in each iteration. Therefore, subsequent models focus more on previously misclassified data points, leading to a refined and accurate prediction.

The advantages of the AdaBoost algorithm can be summarized as follows:

1. High Accuracy: AdaBoost often yields high predictive accuracy compared to individual weak learners. This is because it focuses on misclassified samples and iteratively improves the model's performance.
2. Versatility: AdaBoost can be applied to various types of weak learners, not just decision trees. This makes it adaptable to different types of data and problem domains.
3. Reduced Overfitting: AdaBoost tends to reduce overfitting compared to training a single complex model. It does this by combining multiple weak models, each focusing on different aspects of the data.
4. Handles Noisy Data Well: AdaBoost can handle noisy data and outliers to some extent. Since it gives more weight to misclassified samples, it tends to focus on difficult-to-classify data points.
5. Feature Selection: AdaBoost implicitly performs feature selection by assigning more importance to features that are more informative in the context of the problem.

The disadvantages of the Adaboost algorithm can be summarized as follows:

1. Sensitivity to Noisy Data: While AdaBoost can handle some level of noise, it can still be sensitive to outliers or extremely noisy data. In extreme cases, it may overfit to the noise.
2. Computationally Intensive: Training an AdaBoost model can be computationally intensive, especially when using a large number of weak learners or complex base models.
3. Less Interpretable: The final ensemble model produced by AdaBoost may be less interpretable compared to individual weak models. It may not provide clear insights into the relationships between features and the target variable.
4. Less Effective on Complex Relationships: AdaBoost may struggle with datasets where the underlying relationships are highly complex or not well-captured by simple weak models.
5. Requires Sufficient Data: AdaBoost may not perform well on very small datasets or datasets with insufficient diversity. It relies on a variety of weak models to be effective.

Overall, AdaBoost is a powerful ensemble method that can significantly improve the performance of weak base learners. However, like any ML algorithm, its effectiveness depends on the characteristics of the data and the problem at hand [21].

2.4. ElasticNet

ElasticNet is a linear regression method that combines both L1 (Lasso) and L2 (Ridge) regularization techniques [22]. It is used for variable selection and to mitigate issues arising from multicollinearity in regression analysis. It employs a linear combination of both

L1 and L2 penalties, which allows it to select a subset of important features while still benefiting from the grouping effect of L2 regularization. This is achieved by minimizing the sum of squared differences between observed and predicted values, subject to a penalty term that is a combination of both the L1 and L2 norms of the regression coefficients.

The advantages of the Adaboost algorithm can be summarized as follows:

1. Variable Selection: ElasticNet can perform variable selection by encouraging some of the coefficients to be exactly zero, effectively removing irrelevant features from the model. This is especially beneficial when dealing with high-dimensional datasets, where feature selection is critical.
2. Balancing L1 and L2 Regularization: The α parameter allows for fine-tuning the balance between L1 and L2 regularization. This flexibility enables ElasticNet to capture the advantages of both Lasso (sparsity) and Ridge (stability).
3. Robust to Multicollinearity: ElasticNet can handle multicollinearity, a situation where independent variables are highly correlated, by shrinking and selecting groups of correlated variables simultaneously. This aids in stability and interpretability.
4. Generalization: ElasticNet often yields models that generalize well to new, unseen data. It can prevent overfitting by adding a regularization penalty to the loss function, which is crucial for dealing with noisy or limited data.

The disadvantages of the ElasticNet algorithm can be summarized as follows:

1. Complexity in Choosing Hyperparameters: Selecting appropriate values for hyperparameters can be challenging. The optimal combination depends on the specific problem, and choosing the wrong values may lead to suboptimal results.
2. Computational Cost: Its objective function involves both the L1 and L2 regularization terms, which makes it computationally more expensive than simple linear regression. This cost can be significant for large datasets.
3. Less Interpretability: Although ElasticNet provides a balance between L1 and L2 regularization, the resulting models may be less interpretable than simple linear regression models. This is because some coefficients may be shrunken towards zero or other coefficients, making their individual interpretation less straightforward.

In conclusion, ElasticNet is a powerful regression technique, offering a compromise between Lasso and Ridge regressions. Its ability to handle feature selection, multicollinearity, and regularization makes it a valuable tool in various ML and statistical applications, but careful parameter tuning is required to make the most of its advantages.

2.5. K-Nearest Neighbors

KNN algorithm is a non-parametric and instance-based supervised learning method used for both classification and regression tasks [23]. In this method, the prediction of a target variable for a given data point is determined by identifying the K training examples that are closest to it in the feature space. The predicted value is then computed based on the average (for regression) or majority vote (for classification) of the KNN.

The advantages of the KNN algorithm can be summarized as follows:

1. Simplicity and Intuitiveness: KNN is relatively easy to understand and implement. It does not involve complex mathematical computations or assumptions about the underlying data distribution.
2. No Training Phase: Unlike many other ML algorithms, K-NN does not require a training phase. This means that the model is readily available for prediction once the data is available.
3. Flexibility to Data Distribution: KNN can be applied to both linear and non-linear relationships between features and the target variable. It is not sensitive to the underlying data distribution.
4. Adaptability to New Data: As new data points become available, the KNN model can be easily updated to incorporate this new information.

The disadvantages of the KNN algorithm can be summarized as follows:

1. Computational Complexity: The main computational cost of KNN arises from the need to compute distances between all pairs of data points. As the dataset grows, this can become computationally expensive.
2. Sensitivity to Feature Scaling: The performance of KNN can be influenced by the scale of the features. Therefore, it is essential to normalize or standardize the features before applying this algorithm.
3. Memory Consumption: KNN requires storing the entire training dataset in memory, which can be impractical for very large datasets.
4. Optimal K Selection: Choosing the appropriate value of K (the number of nearest neighbors to consider) can be challenging. A suboptimal choice of K may lead to poor model performance.
5. Imbalanced Data: In classification tasks with imbalanced classes, KNN may be biased towards the majority class since it gives equal weight to all neighbors.
6. Lack of Interpretability: KNN does not provide explicit information on the underlying relationships between features and the target variable. It does not offer coefficients or feature importance scores.
7. Vulnerability to Noisy Data: Outliers and noisy data points can significantly impact the performance of KNN, potentially leading to incorrect predictions.

In summary, while KNN offers simplicity and adaptability to various data distributions, it is important to consider its computational requirements and sensitivity to parameter choices when applying it in practice.

2.6. Gradient Boosting

GB is a powerful ensemble learning technique used in supervised ML tasks, particularly for regression and classification problems [24]. It builds an additive model in a forward stage-wise manner, where each new model attempts to correct the errors made by the previous models. This is achieved by fitting a weak learner, typically a decision tree with limited depth, to the residuals (the differences between the observed and predicted values) of the previous model.

The advantages of the GB algorithm can be summarized as follows:

1. High Predictive Accuracy: GB often yields highly accurate predictions. GB incrementally improves its performance by iteratively addressing the shortcomings of the model, ultimately achieving superior performance compared to individual weak learners.
2. Handles Heterogeneous Data: It is robust to different types of data (categorical or numerical) and can handle a mix of predictor variables effectively.
3. Feature Importance: GB provides a measure of feature importance, indicating which variables are most influential in making accurate predictions.
4. Handles Missing Data: It can handle missing data in a dataset without the need for imputation techniques. It does this by using the information from available predictors.
5. Robust to Outliers: It is less sensitive to outliers in the data compared to other algorithms.

The disadvantages of the GB algorithm can be summarized as follows:

1. Computationally Expensive: Training a gradient boosting model can be computationally expensive, especially when dealing with large datasets and complex weak learners.
2. Prone to Overfitting: Without proper hyperparameter tuning, gradient boosting models can overfit the training data, leading to poor generalization performance on unseen data.
3. Requires Careful Hyperparameter Tuning: Selecting the right hyperparameters is crucial for achieving optimal performance. This process can be time-consuming and may require domain knowledge.

4. Less Interpretable: Unlike simpler models like linear regression, the inner workings of a gradient boosting model are more complex and less interpretable, making it challenging to explain the predictions to non-technical stakeholders.
5. Less Efficient for High-Dimensional Data: GB may not perform as well in situations with a very large number of features, as it may struggle to effectively capture the interactions among them.

In summary, GB is a powerful ensemble learning method known for its high predictive accuracy and versatility in handling different types of data. However, it requires careful parameter tuning and may not be the most efficient choice for very high-dimensional data [25].

3. Experimental Database

This study presents a rigorously curated experimental database encompassing 196 beams, meticulously obtained from 29 conducted experimental studies [26–53]. The experimental database encompasses a comprehensive range of data attributes, including the following parameters: width (b) and effective depth (d) of the concrete beams, concrete compressive strength (f_c), yield strength of steel reinforcement (f_y), transverse steel ratio (A_{sv}), spacing of transverse reinforcement (Sv), shear span to effective depth ratio (a/d), types of fiber employed, and experimental scheme details. Additionally, the database includes information about the types of fiber used, experimental scheme details, as well as the elastic modulus (E_f), ultimate strain (ε_{frp}), tensile strength (f_{frp}), total thickness ($n \times t_f$), width (wf), spacing (sf), height (hf), and angle of inclination (β) of the FRP strips. Lastly, the database also encompasses the shear capacity of beams (V_{exp}). These essential parameters collectively form a comprehensive representation of the experimental data and facilitate a holistic understanding of the shear behavior of concrete beams externally bonded with FRP. Table 1 provides a summary of the collected database. All the mechanical parameters shown in Table 1, except for 'Shear Capacity Contribution by FRP,' are used as prediction inputs. The output of the prediction model is the 'shear capacity contribution by FRP'.

Table 1. Overview of the comprehensive database utilized for AI-based models.

Variables	Notation	Unit	Min	Mean	Std.	Max
Beam Width	b	mm	75.00	180.40	52.02	406.00
Beam Effective Depth	d	mm	120.00	297.40	101.82	660.00
Concrete Compressive Strength	f_c	MPa	13.30	34.13	12.20	71.00
Yield Strength of Steel Reinforcement	f_y	MPa	240.00	458.20	90.47	665.30
Transverse Steel Ratio	A_{sv}	%	0.00	0.12	0.11	0.41
Spacing of Transverse Reinforcement	S_v	mm	0.00	147.70	131.21	400.00
Shear Span to Effective Depth Ratio	a/d	---	1.00	2.78	0.55	4.08
Elastic Modulus of FRP	E_f	GPa	5.30	200.95	109.80	392.00
Ultimate Strain of FRP	ε_{FRP}	---	0.00	0.02	0.01	0.07
Tensile Strength of FRP	f_{FRP}	MPa	112.00	3073.52	1151.52	4500.00
Total Thickness of FRP	$n \times t_f$	mm	0.07	0.38	0.35	1.50
Width of FRP Strips	w_f	mm	1.00	42.94	74.07	304.80
Spacing of FRP Strips	S_f	mm	1.00	124.61	218.08	1195.00
Height of FRP Strips	h_f	mm	150.00	323.52	115.90	720.00
Angle of Inclination of FRP Strips	βeta	°	45.00	84.57	14.62	90.00
Shear Capacity Contribution by FRP	Vexp	kN	3.90	58.86	48.97	343.20

Moreover, the correlation matrix analysis, as depicted in Figure 1, provides valuable insights into the interrelationships between Vexp and the various parameters, offering a comprehensive understanding of the factors influencing the shear capacity contribution by FRP reinforcement in RC beams wrapped with FRP. Among the variables showing positive correlations with V_{exp}, the effective depth (d) exhibits the strongest positive interaction with a coefficient of 0.55, indicating that an increase in the effective depth of the concrete beams is associated with a higher shear capacity contributed by FRP reinforcement. Additionally, the height of FRP strips (h_f) demonstrates a positive correlation with Vexp, with a coefficient of 0.46. Similarly, the width of the beams (b) and the shear span to effective depth ratio (a/d) show positive correlations, with coefficients of 0.40 and 0.20, respectively. Other variables, such as S_v, f_c, n × tf, w_f, f_y, and f_{frp}, also exhibit positive correlations with V_{exp}, albeit with relatively smaller coefficients ranging from 0.01 to 0.13.

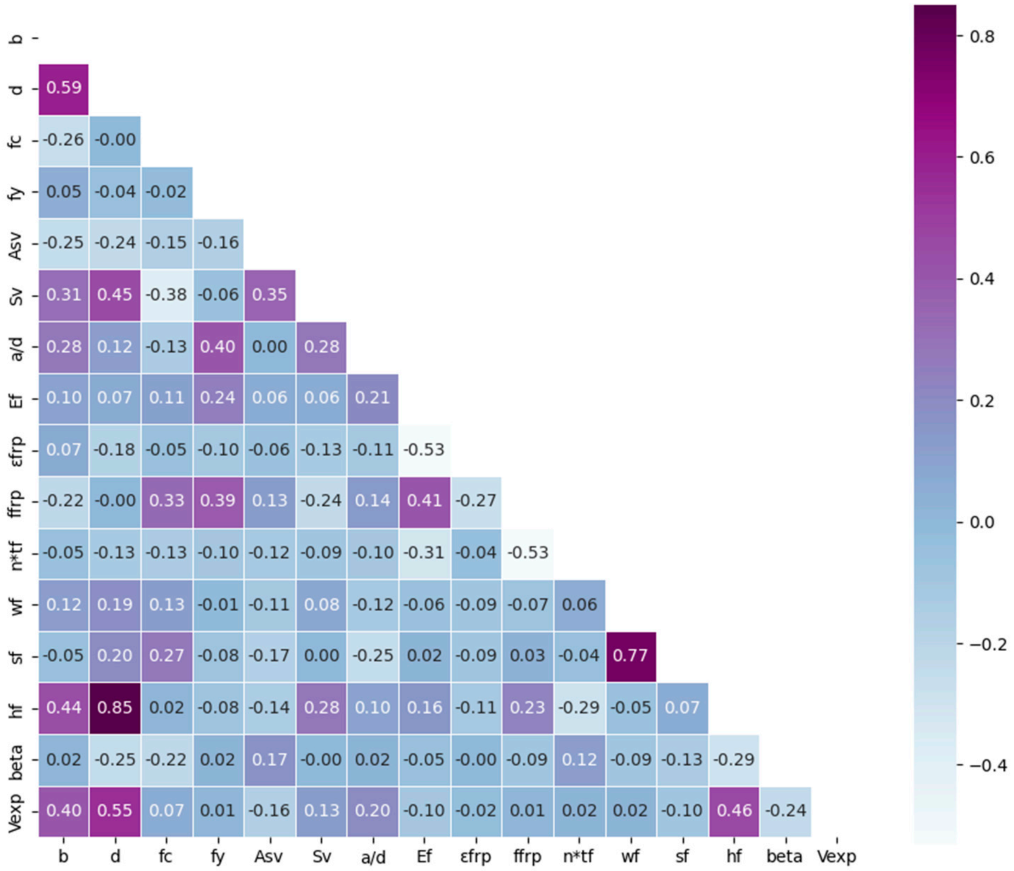

Figure 1. Correlation analysis of FRP-strengthened RC beams.

On the other hand, certain variables display negative correlations with V_{exp}. The ultimate strain of FRP (ε_{frp}) exhibits a negative correlation with a coefficient of −0.02, suggesting that higher ultimate strain values of FRP are associated with a lower shear capacity contribution. Similarly, the spacing of FRP strips (s_f), elastic modulus of FRP (E_f), transverse steel ratio (A_{sv}), and the angle of inclination of FRP strips (β) also show negative correlations with V_{exp}, with coefficients of −0.10, −0.10, −0.16, and −0.24, respectively. These negative correlations indicate that higher values of these variables are associated with a decrease in the shear capacity contributed by FRP reinforcement.

4. AI-Based Analysis

Python was used to perform AI-based analysis, including model training and evaluation. Table 2 presents a comprehensive comparison of the algorithms based on various evaluation metrics. R^2 values for each algorithm obtained indicate the goodness of fit between predicted and actual shear strength values. The Xgboost model achieved the highest R^2 value of 0.901, demonstrating its strong predictive capabilities. This result signifies that approximately 90.1% of the variance in the shear strength can be explained by the Xgboost model. It outperforms other algorithms in terms of predictive accuracy and provides reliable estimations for the shear strength of rectangular RC beams retrofitted with FRP sheets. The GB algorithm also exhibits satisfactory performance with an R^2 value of 0.828. This value indicates that around 82.8% of the variability in the shear strength can be attributed to the predictions of the GB model. Although slightly lower than Xgboost, it still demonstrates a strong correlation between the predicted and observed shear capacity values. The RF and AdaBoost models yielded R^2 values of 0.747 and 0.746, respectively. These values indicate that these models can explain approximately 74.7% and 74.6% of the variability in shear strength, respectively. While these algorithms are reasonably good predictors, they have a slightly lower correlation than Xgboost and GB. The R^2 values for the KNN and ElasticNet algorithms, on the other hand, are 0.506 and 0.468, respectively. These values indicate that the predictions from these models explain approximately 50.6% and 46.8% of the variability in shear strength, respectively. These algorithms have lower predictive capabilities than the other models.

Table 2. Evaluation metrics for algorithm comparison.

Model	RMSE	MSE	MAE	R^2
XGBoost	20.065	402.608	13.856	0.901
GB	26.454	699.823	18.427	0.828
RF	32.148	1033.504	21.275	0.747
AdaBoost	32.163	1034.457	24.163	0.746
KNN	44.888	2014.893	26.398	0.506
Elastic Net	46.566	2168.379	30.654	0.468

Additional evaluation metrics, such as Root Mean Squared Error (RMSE), Mean Squared Error (MSE), and Mean Absolute Error (MAE), were computed to further assess the performance of the algorithms. The RMSE values calculate the average difference between predicted and actual shear strength values. The lower the RMSE, the more precise the predictions. The Xgboost model had the lowest RMSE of 20.065, followed by the GB model, which had an RMSE of 26.454. The RMSE values for the RF and AdaBoost models were 32.148 and 32.163, respectively. The KNN and ElasticNet algorithms demonstrated higher RMSE values of 44.888 and 46.566, respectively. These values suggest that the Xgboost and GB models yield more precise predictions compared to the other algorithms. Additionally, the MSE values were calculated to quantify the overall prediction error. The Xgboost model yielded the lowest MSE value of 402.608, followed by the GB model with a value of 699.823. MSE values for the RF and AdaBoost models were 1033.504 and 1034.457, respectively. KNN and ElasticNet algorithms had higher MSE values of 2014.893 and 2168.379, respectively. Furthermore, the MAE values were calculated to determine the average absolute difference between the predicted and actual shear strength values. The Xgboost model demonstrated the lowest MAE value of 13.856, followed by the GB model with a value of 18.427. The RF and AdaBoost models yielded MAE values of 21.275 and 24.163, respectively. The KNN and ElasticNet algorithms resulted in higher MAE values of 26.398 and 30.654, respectively. These metrics collectively demonstrate the superior performance of the Xgboost model, followed by GB, RF, and AdaBoost models, while KNN and ElasticNet exhibit relatively lower predictive accuracy. The performance comparison is visually depicted in Figure 2, where bar plots illustrate the MAE, MSE, R^2 Score, and RMSE values for each model.

Figure 3 provides a visual representation of the relationship between the predicted and actual shear strength values for rectangular RC beams wrapped with FRP sheets using a range of ML algorithms. The x-axis represents the true shear strength values in kilonewtons (kN), while the y-axis represents the predicted shear strength values. The scatter plot serves as a visual representation of the extent to which the predicted values align with the actual values. Ideally, a perfect alignment would result in a cluster of data points tightly distributed along the diagonal line, indicating a high degree of concordance between the predicted and experimental shear strength values. Conversely, greater dispersion and deviations from the diagonal line signify a weaker correlation and less accurate predictions.

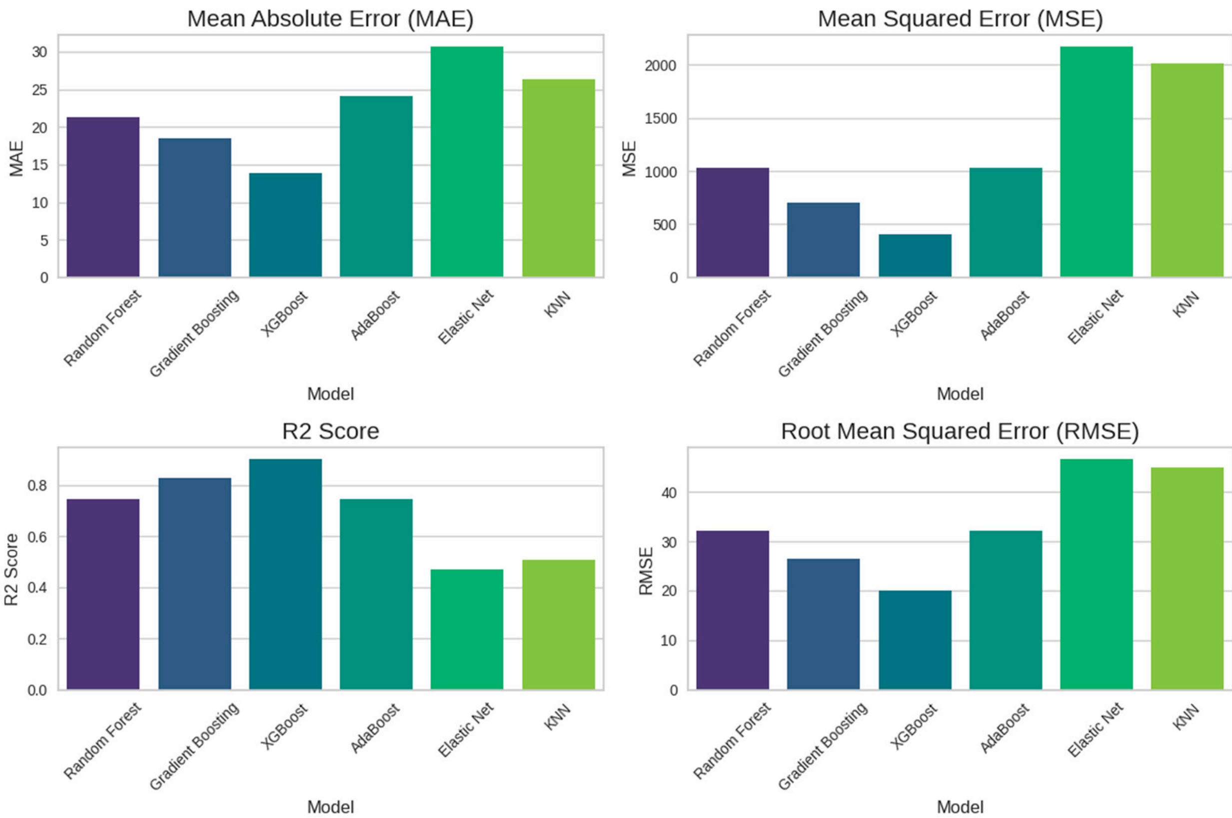

Figure 2. Visual representation of model performance evaluation.

Upon careful examination of the scatter plot, it becomes evident that the Xgboost model exhibits the most remarkable predictive capabilities among the examined algorithms. The data points cluster densely around the diagonal line, implying a substantial agreement between the predicted and actual shear strength values. This noteworthy alignment underscores the Xgboost model's capacity to discern underlying patterns within the dataset and provide reliable predictions for the shear strength of the beams wrapped with FRP sheets. Likewise, the GB algorithm demonstrates a reasonably strong correlation between the predicted and observed values, albeit somewhat less precise when compared to Xgboost. The data points exhibit a moderate clustering pattern around the diagonal line, indicating that the GB model adeptly captures the inherent relationships within the data, thereby yielding predictions of shear strength with a commendable level of accuracy. Regarding the RF and AdaBoost algorithms, the scatter plot exhibits a moderate alignment between the predicted and actual values. Although there are some deviations from the diagonal line, the overall clustering of data points suggests that the RF and Adaboost models can provide reasonably accurate predictions for shear strength estimation. However, for the KNN, and ElasticNet algorithms, the scatter plots indicate less pronounced alignments between the predicted and actual values. The data points exhibit more significant deviations from the diagonal line, indicating a weaker correlation and less accurate predictions for the shear strength of the beams. In summary, the scatter plot figure validates the R^2 values obtained for each algorithm, further emphasizing the performance of the Xgboost algorithm in accurately predicting the shear strength of rectangular RC beams strengthened with FRP sheets. The GB, RF, and AdaBoost models also show promising performance while the KNN and ElasticNet algorithms exhibit relatively lower predictive accuracy.

The analysis of prediction errors, visually depicted in Figure 4, yields valuable insights into the efficacy of the ML algorithms in accurately estimating the shear strength of rectangular RC beams bonded with FRP sheets. Figure 4 illustrates the disparity between the predicted and actual shear strength values. Remarkably, the Xgboost model exhibits significantly smaller prediction errors compared to the other algorithms, indicating its superior predictive capabilities. This observation substantiates previous findings, underscoring the Xgboost model's exceptional accuracy in estimating the shear strength of rectangular RC beams wrapped with FRP sheets. Conversely, the remaining models demonstrate comparatively larger prediction errors, suggesting relatively less precise predictions.

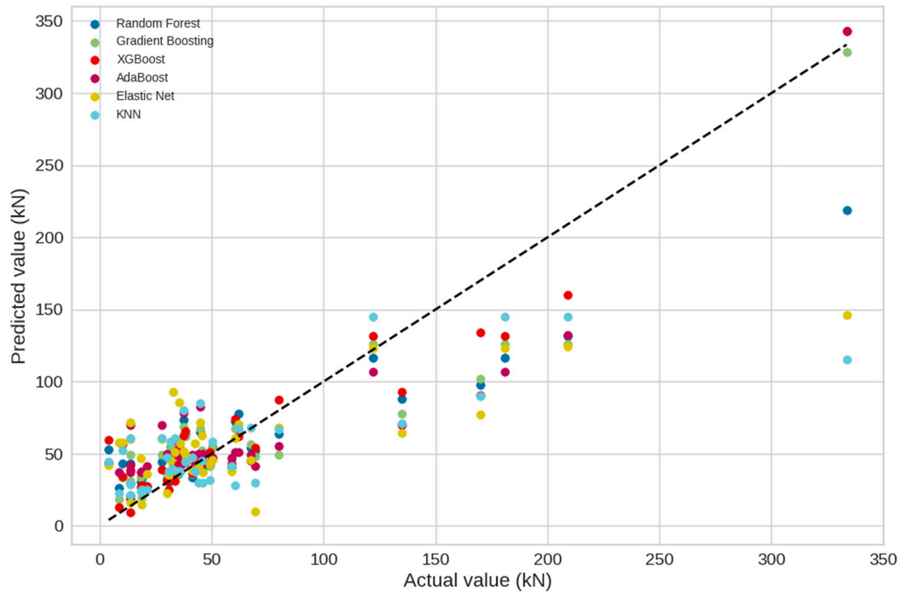

Figure 3. Comparison of predicted and actual shear strength in FRP-strengthened RC beams.

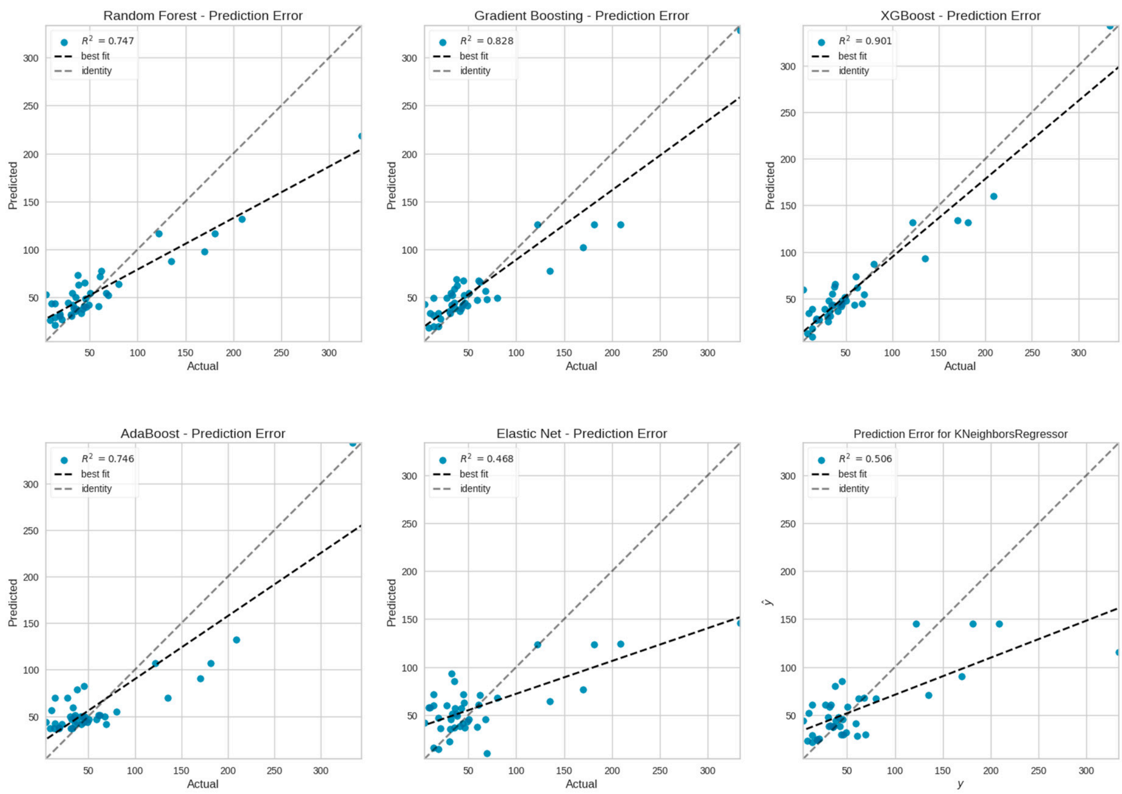

Figure 4. Comparative analysis of prediction errors in shear strength estimation for FRP-strengthened RC beams.

Under careful examination of Figure 5, depicting the residuals, we delve into the analysis of the disparities between the predicted and experimental values. Consistently, the Xgboost model displays the smallest residuals, with values closer to zero, indicating minimal bias in its predictions. In contrast, the residuals for the other models exhibit a broader distribution, implying a higher degree of variability and potential bias in their predictions.

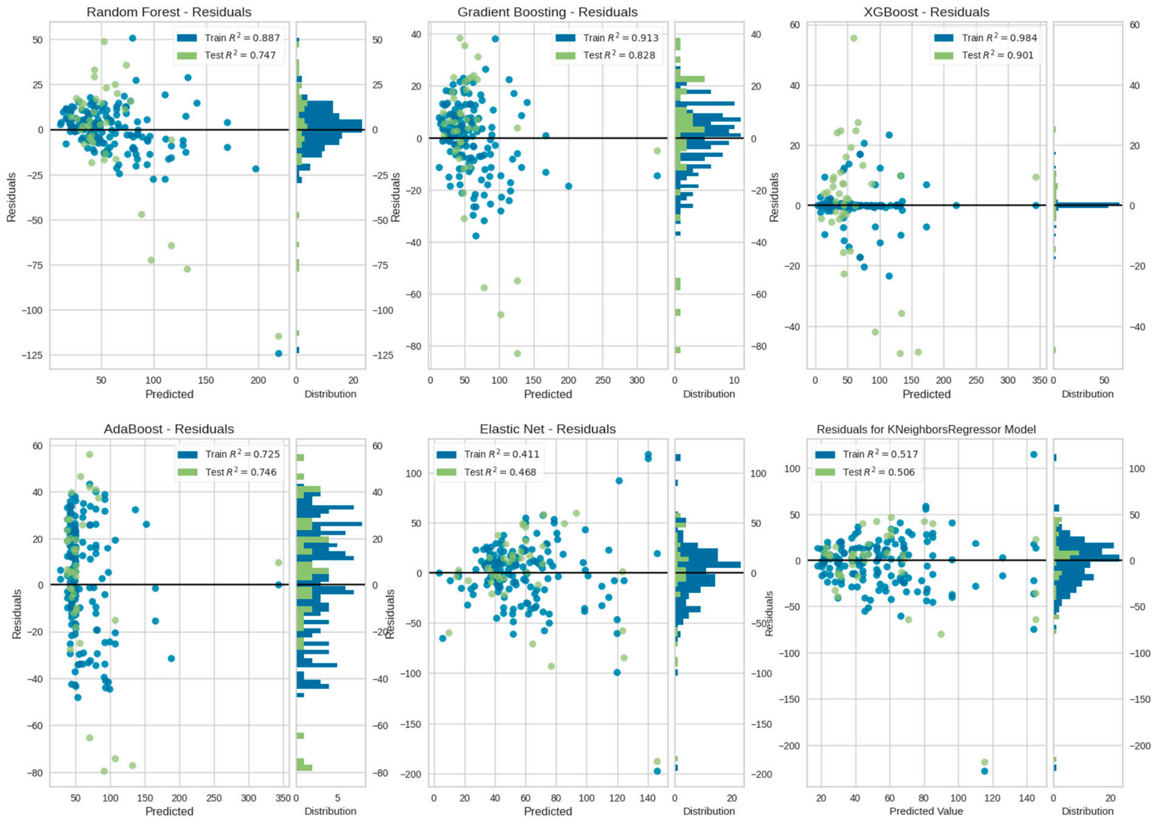

Figure 5. Residual analysis of predicted vs. actual values in Shear strength estimation for FRP-strengthened concrete beams.

Overall, the visual analysis of the prediction error and residual plots aligns with the earlier quantitative evaluation metrics, further validating the superior performance of the Xgboost model. The smaller prediction errors and tighter distribution of residuals observed for Xgboost provide strong evidence of its ability to accurately capture the underlying patterns in the dataset. Consequently, the Xgboost model emerges as a reliable tool for predicting the shear strength of rectangular RC beams wrapped with FRP sheets, offering significant practical utility in engineering applications.

It is important to note that these visual representations serve as complementary evidence to the previously discussed numerical evaluation metrics. Together, they provide a thorough assessment of the models' performance and support the conclusion that the Xgboost model excels as the most accurate and reliable predictor in this study.

The analysis of the residual distribution, as depicted in Figure 5, provides further understanding of the models' performance in predicting the shear strength of the beams. The histograms in Figure 6 showcase the distribution patterns of the residuals for each model. The shape, spread, and central tendency of the residuals offer crucial information regarding the accuracy and precision of the predictions made by the models. Examining the histograms, we observe that the residuals exhibit varying distributions for different models. A desirable characteristic is a distribution centered around zero, indicating minimal bias in the predictions. Additionally, a narrower spread of the residuals implies higher precision in the model's predictions. In the visual representation, alongside the colored lines, multiple rectangular boxes are present along the x-axis (residuals), each corresponding to a specific algorithm employed in the analysis. The positioning of these boxes along the x-axis provides insight into the distribution and magnitude of residuals for each algorithm. A lower placement along the *y*-axis suggests a higher density of residuals, while a higher placement indicates a lower density. In essence, a box located lower on the *y*-axis signifies a more concentrated distribution of residuals for that particular algorithm.

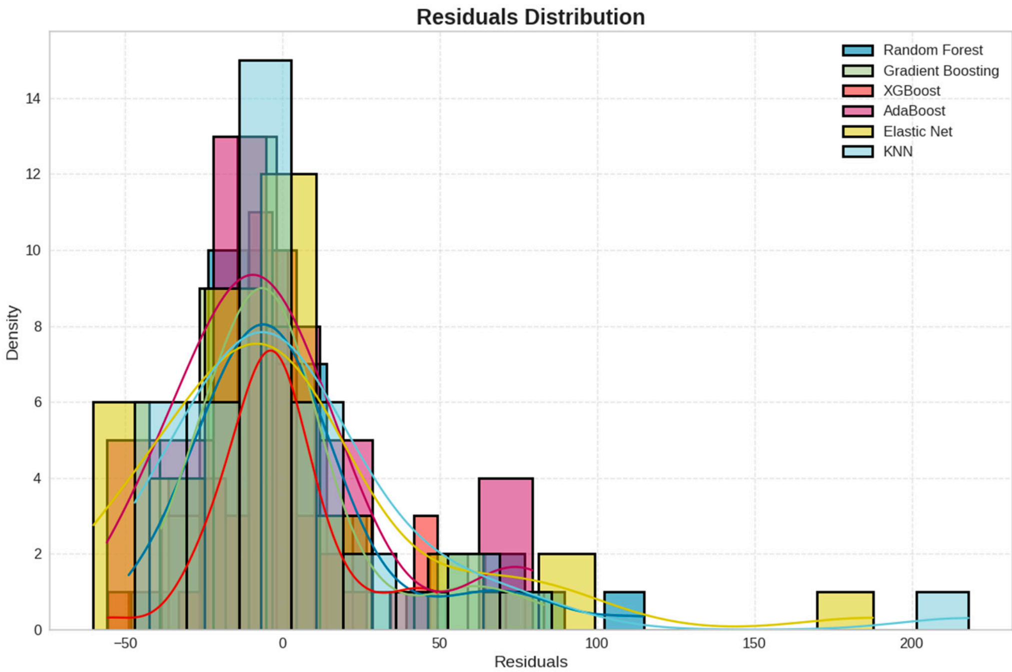

Figure 6. Distribution analysis of residuals in shear strength prediction for FRP-strengthened beams.

To aid in clarity, a colored line is assigned to each algorithm. The position of the colored lines serves as an additional visual cue to interpret the overall performance of each algorithm. A colored line positioned lower along the *y*-axis and with a shorter span along the *x*-axis suggests fewer and more concentrated residuals. For example, the red line representing the XGBoost algorithm is located at the bottom of the *y*-axis and exhibits a narrow span along the *x*-axis, indicating a lower density and more accurate predictions.Comparing the histograms, we find that the Xgboost model demonstrates a distribution of residuals that is more concentrated around zero, suggesting reduced bias and improved accuracy. This aligns with the previous evaluation metrics, reinforcing the notion that the Xgboost model outperforms the other models in predicting the shear strength of rectangular RC beams wrapped with FRP sheets. Conversely, the histograms for the remaining models exhibit wider distributions of residuals, indicating a relatively higher degree of variability and potential bias in their predictions. The insights gained from the analysis of Figure 6 further corroborate the superiority of the Xgboost model in accurately estimating the shear strength. Its ability to generate predictions with smaller residuals and a narrower distribution underscores its capacity to capture the underlying patterns in the data more effectively. Overall, the examination of the distribution of the residuals depicted in Figure 6 supports and reinforces the conclusion that the Xgboost model is the most accurate and reliable predictor among the models evaluated in this study.

5. Sensitivity Analysis by ANN

Numerous approaches exist for depicting the significance of input parameters concerning the target variable. For instance, Zaitseva et al. [54] introduced a novel method for assessing the importance of attributes in classification tasks. The study acknowledges that various factors and input data quality can influence the effectiveness of classification techniques. Their method, based on Importance Analysis from reliability engineering, measures the sensitivity of input attributes in the classification process, highlighting which attributes have the most significant impact on classification results. The importance of attributes is determined using a specialized index known as structural importance. The authors demonstrate the method's application using a Fuzzy Decision Tree, which considers uncertainty in the initial data, but it is adaptable for use with other classifiers as well.

Determining the relative importance of input variables on selected outputs can be achieved by analyzing neural network weights. Neural networks employ weights to quantify the contribution of each input variable to the final output. These weights represent the strength of connections between the input variables and the neurons in the network's hidden layers. To assess the relative importance of input variables using neural network weights, the first step is to train the neural network. During the training process, the weights are adjusted iteratively to minimize the error between predicted outputs and experimental outputs. Once the network is trained, the weights associated with each input variable can be examined.

The magnitude of the weights is indicative of the relative importance of the corresponding input variables. Larger weights suggest a stronger influence of the input variable on the output. Positive weights indicate a positive relationship, while negative weights signify a negative relationship. It is often beneficial to normalize the weights before comparing their relative importance. Normalization techniques, such as dividing the weights by their sum or scaling them to a specific range, can facilitate fair comparisons between variables. By analyzing the weights, one can rank or compare them to identify the input variables with the highest relative importance. Variables with higher weights are considered more influential in determining the output. However, it is essential to exercise caution when interpreting neural network weights. The relationship between weights and the importance of input variables can be complex and nonlinear. Additionally, other factors such as network architecture, activation functions, and regularization techniques can influence the interpretation. Therefore, it is advisable to combine weight analysis with other techniques to obtain a comprehensive understanding of variable importance. In this regard, an ANN was created using all the input and target data. After training the data and satisfying the criteria, its results were utilized for sensitivity analysis. A flowchart of artificial neural networks representing its working algorithm is presented in Figure 7. Table 3 presents the weights obtained from the idealized neural network. The results of the sensitivity analysis are summarized in Figure 8, which reflects the relative importance of each input data.

Table 3. Weights obtained from the idealized neural network.

0.488	0.610	−0.507	0.773	0.200	−0.900	−0.398	0.161	0.628	0.339
−0.568	0.373	0.565	−0.035	0.186	−0.649	−0.325	1.181	0.249	0.394
0.280	−0.685	0.454	0.470	0.172	0.384	0.297	−0.417	0.138	−0.516
0.203	−0.620	0.107	−0.345	−0.699	0.334	0.495	0.134	0.658	−0.210
−0.026	−0.399	0.359	0.285	−0.452	0.166	0.012	0.367	0.324	0.278
−0.328	−0.270	0.029	−0.206	−0.502	−0.023	1.001	−0.399	−0.083	−0.329
0.301	−0.854	0.384	0.747	0.323	0.568	0.032	−0.214	−0.589	−0.294
0.606	−0.382	0.399	−0.248	0.587	−0.321	−0.320	−0.694	0.107	−0.094
−0.277	0.500	0.175	0.380	0.457	−0.169	0.382	0.251	−0.106	0.000
−0.626	−0.364	−0.095	0.269	0.481	−0.408	0.317	−0.250	−0.707	0.030
−0.680	0.071	−0.006	−0.016	−0.595	0.332	−0.663	0.349	−0.033	0.424
−0.020	−0.388	−0.475	0.121	−0.295	0.208	0.311	0.428	−0.651	0.137
−0.661	0.647	−0.695	0.681	0.509	0.346	−0.461	−0.331	−0.514	0.731
−0.069	0.541	−0.792	−0.381	−0.564	−0.356	0.725	0.354	0.047	−0.382
0.701	0.078	−0.238	0.048	−0.338	−0.410	−0.177	−0.569	−0.456	−0.417
−0.148	−0.499	0.239	0.768	−0.200	−0.336	−0.309	0.683	−0.248	−0.545

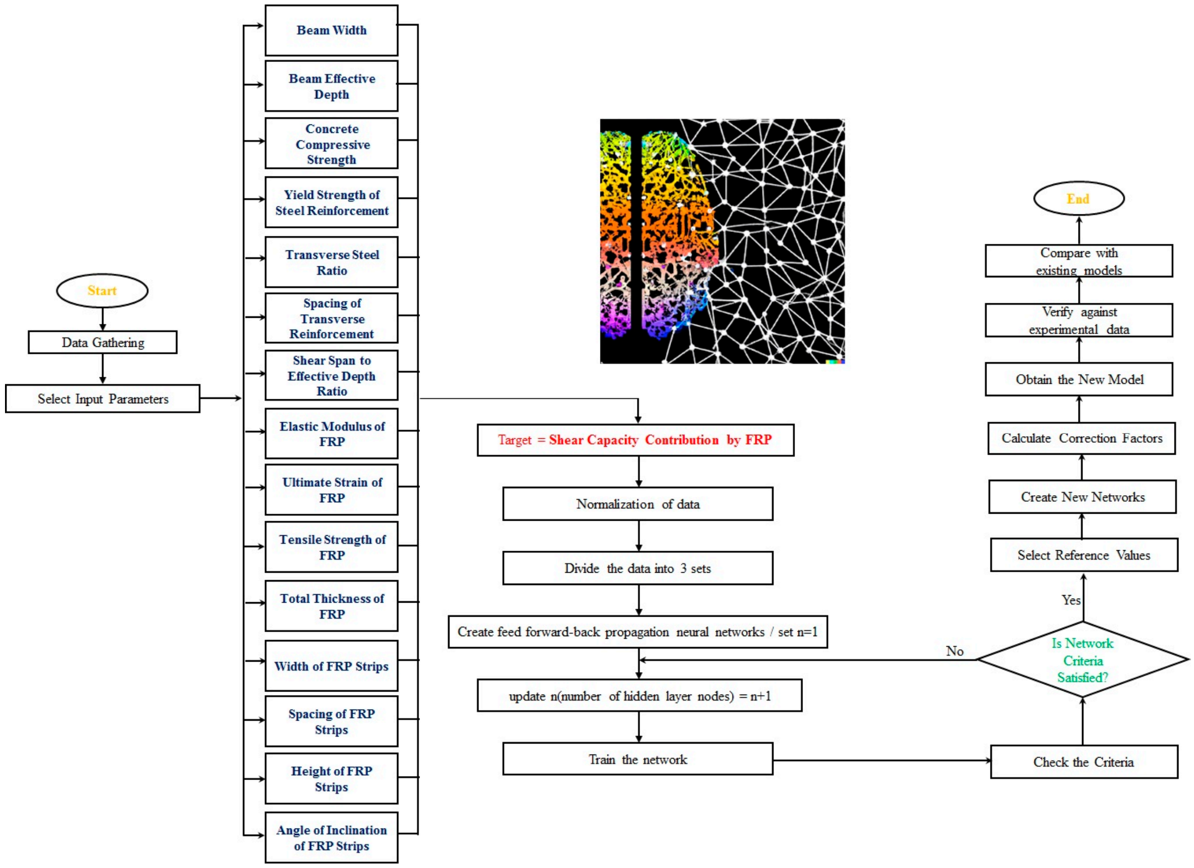

Figure 7. Flowchart of artificial neural networks used in this study.

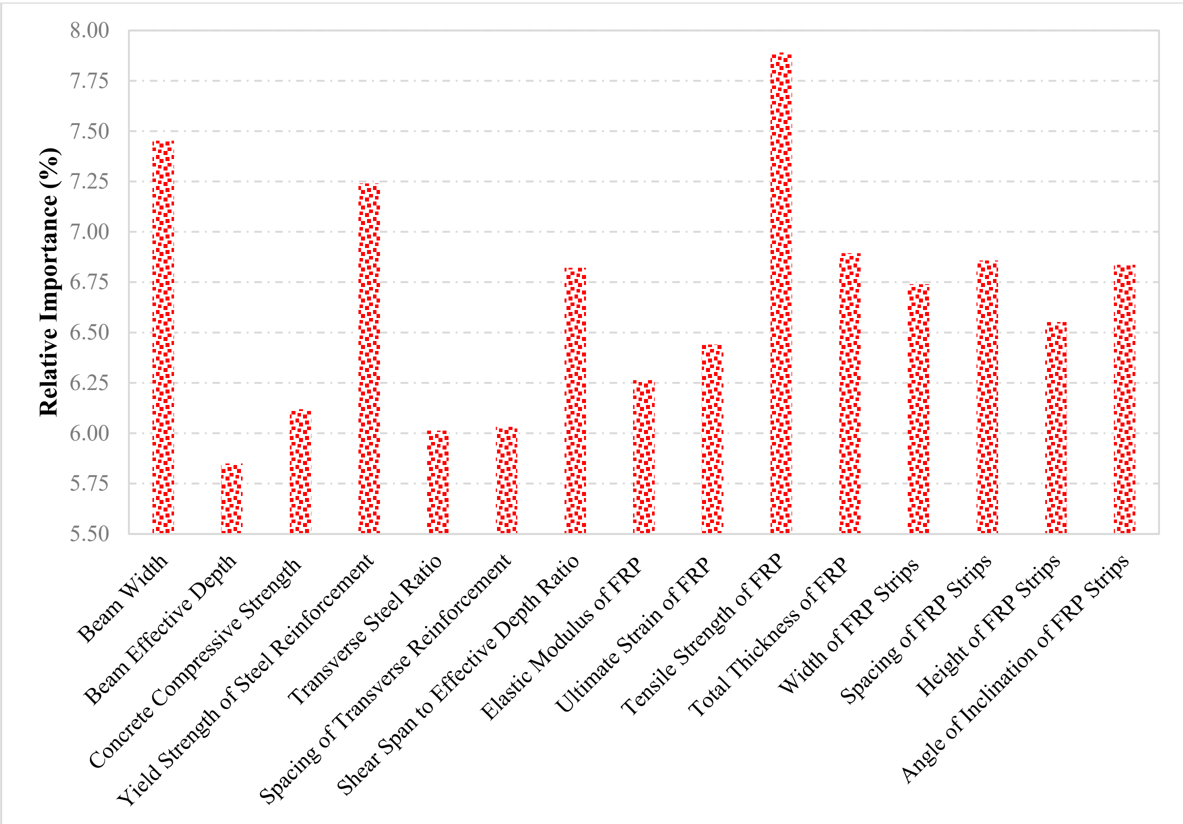

Figure 8. Relative importance of input parameters.

The results indicated that four parameters, including the tensile strength of FRP, yield strength of steel reinforcement, beam width, and total thickness of FRP, have a profound impact on the output as they directly influence the structural behavior and performance of the system.

The FRP material's tensile strength is a significant factor in determining the output. It denotes the FRP's ability to withstand tension and is critical in maintaining structural integrity and load-bearing capacity. FRP with a higher tensile strength has better reinforcement effectiveness and overall structural performance. The yield strength of the steel reinforcement is a vital parameter that greatly impacts the structural performance. It determines the maximum stress level at which the steel can undergo elastic deformation without permanent deformation. A higher yield strength enables greater load-bearing capacity and resistance to yielding, resulting in a more structurally robust system. The width of the beam is an important factor that has a significant impact on the output. It has a direct impact on the load-carrying capacity, stiffness, and behavior of the beam, as well as the overall structural performance. A wider beam offers increased resistance to bending and enhances the structural performance, making it a key parameter in achieving desired output goals. The total thickness of the FRP material is a significant parameter in structural reinforcement. It is crucial in determining the FRP system's strength, stiffness, and durability. A thicker FRP layer improves the load-carrying capacity and overall performance of the strengthened structure, thereby contributing to the desired output objectives.

It is worth emphasizing the importance of FRP properties in influencing the output. The tensile strength of FRP and the total thickness of FRP are two of the most influential parameters in determining structural performance. The high tensile strength of FRP enables it to effectively resist tension and enhance the load-bearing capacity of structures. Additionally, increasing the thickness of the FRP layer contributes to improved structural stiffness and strength, making FRP an invaluable material for reinforcing and retrofitting applications. These FRP properties have a significant impact on the output by ensuring structural integrity, durability, and overall performance.

6. Conclusions

A comprehensive investigation into accurately predicting the shear strength of FRP-strengthened RC beams using sophisticated ML algorithms was conducted. The evaluation and comparison of various algorithms, including Xgboost, GB, RF, AdaBoost, KNN, and ElasticNet, provide valuable insights into their predictive performance.

The extensive experimental database curated in this study, encompassing 196 beams and a comprehensive range of data attributes, is a valuable resource for the research community and practitioners. The experimental database comprises a wide spectrum of data attributes, encompassing key parameters such as the dimensions of the concrete beams, concrete compressive strength, yield strength of steel reinforcement, transverse steel ratio, spacing of transverse reinforcement, shear span to effective depth ratio, types of fiber employed, experimental scheme details, as well as the elastic modulus, ultimate strain, tensile strength, total thickness, width, spacing, height, and angle of inclination of the FRP strips.

The evaluation metrics employed, namely R^2, RMSE, MSE, and MAE, served as robust measures for assessing the accuracy and precision of the algorithms. Among the evaluated algorithms, the Xgboost model demonstrated outstanding performance, exhibiting the highest R^2 score and the lowest RMSE and MAE values. These findings establish the superiority of the Xgboost algorithm in terms of its predictive capabilities compared to the other algorithms studied. The scatter plot analysis further emphasizes the remarkable predictive capabilities of the Xgboost model, with data points clustering closely around the diagonal line, indicating a high degree of concordance between the predicted and observed values. The analysis of prediction errors and residuals supports the superior performance of the Xgboost model, revealing smaller prediction errors and a narrower distribution of residuals, indicative of reduced bias and increased accuracy.

Furthermore, a sensitivity analysis was performed using Artificial Neural Networks (ANNs) to quantify the impact of input variables on shear strength prediction. By analyzing the weight assignments associated with each input variable in the trained neural networks, a precise evaluation was made regarding the relative contributions of these variables to the output. Significantly, the tensile strength of FRP, yield strength of steel reinforcement, beam width, and total thickness of FRP emerged as influential factors directly influencing the structural behavior and performance.

Future research endeavors can focus on expanding the dataset and exploring additional variables to further refine the predictive models and broaden their applicability in practical scenarios. Additionally, investigating alternative ML algorithms and incorporating hybrid approaches may provide further improvements in predictive accuracy. This research paves the way for improved prediction models and practical applications in engineering design and analysis involving FRP-strengthened structures, advancing the field and facilitating more efficient and reliable structural solutions.

Author Contributions: N.E., H.N., and A.Ö.Ç.: conceptualization; H.N., A.Ö.Ç. and M.M.: data curation; A.Ö.Ç.: formal analysis; N.E., H.N. and A.Ö.Ç.: investigation; N.E., H.N. and A.Ö.Ç.: methodology; H.N. and A.Ö.Ç.: project administration; N.E., H.N., A.Ö.Ç. and M.M.: software; H.N.: supervision; H.N., A.Ö.Ç. and M.M.: validation; N.E., H.N. and A.Ö.Ç.: visualization; N.E., H.N., A.Ö.Ç. and M.M.: roles/writing—original draft; N.E., H.N. and A.Ö.Ç.: writing—review and editing. All authors have read and agreed to the published version of the manuscript.

Funding: This research received no external funding.

Institutional Review Board Statement: Not Applicable.

Informed Consent Statement: Not Applicable.

Data Availability Statement: The data used to support the findings of this study are included within the article.

Conflicts of Interest: Author Nima Ezami was employed by the company GEI Consultants Inc. The remaining authors declare that the research was conducted in the absence of any commercial or financial relationships that could be construed as a potential conflict of interest.

Appendix A

Table A1. Experimental Data of Rectangular RC Beams Strengthened with FRP.

No	b	d	f_c	f_y	A_{sv}	S_v	a/d	FRP Type	Scheme	Ef	εfrp	ffrp	n^*t_f	wf	sf	hf	beta	Vexp
1	250	420	13.3	500	0.096	400	3.33	CFRP	U	390	0.008	3000	0.22	150	225	450	45	66.5
2	250	420	13.3	500	0.096	400	3.33	CFRP	U	390	0.008	3000	0.22	1	1	450	90	27
3	250	420	13.3	500	0.096	400	3.33	CFRP	U	390	0.008	3000	0.22	150	300	450	60	13
4	250	420	13.3	500	0.096	400	3.33	CFRP	U	390	0.01	3000	0.22	150	300	450	45	28
5	250	420	13.3	500	0.096	400	3.33	CFRP	U	390	0.008	3000	0.22	50	100	450	45	35.5
6	200	380	35.1	500	0.074	400	3.29	CFRP	U	240	0.013	3500	0.11	100	400	450	90	41.2
7	200	395	36.8	500	0.072	400	3.29	CFRP	U	240	0.013	3500	0.11	50	400	450	90	33.4
8	200	395	35.8	500	0.072	400	3.29	CFRP	U	240	0.013	3500	0.11	50	600	450	90	30
9	150	255	19.3	350	0.41	125	2.98	CFRP	SB	228	0.017	3790	0.33	1	1	305	90	50.5
10	150	255	19.3	350	0.41	125	4	CFRP	SB	228	0.017	3790	0.33	50	125	305	90	80.5
11	150	255	27.5	460	0	0	2.98	CFRP	U	228	0.017	3790	0.165	1	1	305	90	54
12	150	255	27.5	460	0	0	2.98	CFRP	U	228	0.017	3790	0.33	1	1	305	90	92.5
13	150	255	27.5	460	0	0	2.98	CFRP	U	228	0.017	3790	0.165	50	125	305	90	67.5
14	150	255	27.5	460	0	0	4	CFRP	U	228	0.017	3790	0.165	1	1	305	90	62.5
15	150	255	27.5	460	0	0	4	CFRP	U	233.6	0.016	4490	0.165	1	1	305	90	90.5
16	150	250	22.82	548	0	0	3	CFRP	SB	233.6	0.019	4490	0.165	1	1	300	90	45.3
17	150	250	22.82	548	0	0	3	CFRP	SB	233.6	0.019	4490	0.495	1	1	300	90	38.1
18	150	250	22.82	548	0	0	3	CFRP	SB	233.6	0.019	4490	0.495	1	1	300	90	65.5
19	150	250	26.06	548	0.268	200	3	CFRP	SB	233.6	0.019	4490	0.33	1	1	300	90	31.5
20	150	250	26.06	548	0.268	200	3	CFRP	SB	233.6	0.019	4490	0.495	1	1	300	90	51.8

Table A1. *Cont.*

No	b	d	f_c	f_y	A_{sv}	S_v	a/d	FRP Type	Scheme	Ef	εfrp	ffrp	n^*t_f	wf	sf	hf	beta	Vexp
21	150	250	26.06	548	0.268	200	3	CFRP	SB	233.6	0.019	4490	0.495	1	1	300	90	86
22	150	250	26.06	548	0.268	200	3	CFRP	SB	233.6	0.019	4490	0.33	1	1	300	90	47.3
23	150	250	26.06	548	0.268	200	3	CFRP	SB	233.6	0.019	4490	0.33	1	1	300	90	50.5
24	300	245	37.2	395	0	0	4.08	CFRP	U	230	0.015	3400	0.167	1	1	300	90	53
25	300	245	41	395	0	0	4.08	CFRP	U	230	0.015	3400	0.167	1	1	300	90	116.5
26	300	245	41.1	395	0	0	4.08	CFRP	U	230	0.015	3400	0.167	1	1	300	90	125.5
27	130	425	38	240	0.102	300	2.12	CFRP	F	105	0.013	1400	0.43	40	200	450	90	135
28	130	425	38	240	0.102	300	2.12	CFRP	F	105	0.013	1400	0.43	40	250	450	90	90
29	130	425	38	240	0.102	300	2.12	CFRP	F	105	0.013	1400	0.43	40	300	450	45	71
30	130	425	38	240	0.102	300	2.12	CFRP	F	105	0.013	1400	0.43	40	350	450	45	44
31	130	425	38	240	0.102	300	2.12	CFRP	U	105	0.013	1400	0.43	40	200	450	90	65
32	130	425	38	240	0.102	300	2.12	CFRP	U	105	0.013	1400	0.43	40	250	450	90	40
33	130	425	38	240	0.102	300	2.12	CFRP	U	105	0.013	1400	0.43	40	300	450	45	89
34	130	425	38	240	0.102	300	2.12	CFRP	U	105	0.013	1400	0.43	40	350	450	45	80
35	150	170	35.4	582	0	0	3	CFRP	SB	230	0.015	3400	0.167	1	1	200	90	11.3
36	150	170	33.5	582	0	0	3	CFRP	SB	230	0.015	3400	0.334	1	1	200	90	24.4
37	150	170	31.5	582	0	0	3	CFRP	SB	230	0.015	3400	0.167	1	1	200	90	19.4
38	150	170	31	582	0	0	3	CFRP	SB	230	0.015	3400	0.334	1	1	200	90	21.1
39	150	170	33.7	582	0	0	3	CFRP	SB	230	0.015	3400	0.334	1	1	200	90	41.6
40	150	170	34.4	582	0	0	3	CFRP	U	230	0.015	3400	0.167	1	1	200	90	29.3
41	150	170	35.4	582	0	0	3	CFRP	U	230	0.015	3400	0.167	1	1	200	90	46.6
42	150	296	41.03	494.5	0.127	160	3.04	GFRP	F	75.9	0.047	3600	0.12	1	1	350	90	56
43	150	296	41.03	494.5	0.127	160	3.04	GFRP	F	75.9	0.047	3600	0.24	1	1	350	90	84
44	150	296	41.03	494.5	0.127	160	3.04	GFRP	F	75.9	0.047	3600	0.36	1	1	350	90	93
45	150	222.5	30.5	303	0.169	200	2.7	CFRP	F	249	0.015	3635	0.167	30	100	250	90	44
46	150	222.5	30.5	303	0.169	200	2.7	CFRP	F	249	0.015	3635	0.167	30	150	250	90	46
47	150	222.5	30.5	303	0.169	200	1.8	CFRP	F	249	0.015	3635	0.167	30	100	250	90	44
48	150	222.5	30.5	303	0.169	200	1.8	CFRP	F	249	0.015	3635	0.167	30	50	250	90	34
49	150	222.5	30	361	0	0	2.47	GFRP	F	20.5	0.013	260	1.27	20	40	250	90	70
50	150	222.5	30	361	0	0	2.47	GFRP	F	20.5	0.013	260	1.27	20	80	250	90	55
51	150	222.5	30	361	0	0	1.35	GFRP	F	20.5	0.013	260	1.27	20	40	250	90	28
52	150	222.5	30	361	0	0	1.35	GFRP	F	20.5	0.013	260	1.27	20	80	250	90	11
53	150	222.5	17.8	361	0	0	2.92	GFRP	F	5.3	0.021	112	1.2	25	50	250	90	40
54	150	222.5	17.8	361	0	0	2.92	GFRP	F	5.3	0.021	112	1.2	25	100	250	90	35
55	150	222.5	17.8	361	0	0	1.8	GFRP	F	5.3	0.021	112	1.2	25	50	250	90	47
56	150	222.5	17.8	361	0	0	1.8	GFRP	F	5.3	0.021	112	1.2	25	100	250	90	35
57	180	426	67	500	0	0	2.93	CFRP	SB	234	0.019	4500	0.072	1	1	500	45	122
58	180	426	59	500	0	0	2.93	CFRP	SB	234	0.019	4500	0.11	1	1	500	45	29
59	180	426	71	500	0	0	2.93	CFRP	SB	234	0.019	4500	0.11	1	1	500	45	132
60	180	426	53	500	0	0	2.93	CFRP	SB	234	0.019	4500	0.11	1	1	500	45	180
61	180	426	67	500	0	0	2.93	CFRP	SB	234	0.019	4500	0.11	1	1	500	45	181
62	180	426	47	500	0	0	2.93	CFRP	SB	234	0.019	4500	0.11	1	1	500	45	126
63	180	426	53	500	0	0	2.93	CFRP	SB	234	0.019	4500	0.11	1	1	500	45	166
64	180	426	71	500	0	0	2.93	CFRP	SB	234	0.019	4500	0.165	1	1	500	45	209
65	180	426	54	500	0	0	2.93	CFRP	SB	234	0.019	4500	0.165	1	1	500	45	219
66	180	335	46	500	0.094	200	2.99	CFRP	SB	234	0.019	4500	0.165	1	1	400	90	62
67	180	335	46	500	0.094	200	2.99	CFRP	SB	234	0.019	4500	0.165	1	1	400	90	62
68	152.4	189.1	43.8	400	0	0	2.82	CFRP	SB	165	0.017	2800	1.5	40	127	228.6	90	27.6
69	152.4	189.1	43.8	400	0	0	2.82	CFRP	SB	165	0.017	2800	1.5	6	127	228.6	45	36.7
70	152.4	189.1	43.8	400	0	0	2.5	CFRP	SB	165	0.017	2800	1	1	1	228.6	90	7.5
71	152.4	189.1	43.8	400	0	0	2.5	CFRP	SB	165	0.017	2800	1.5	40	127	228.6	90	21
72	152.4	189.1	43.8	400	0	0	2.5	CFRP	SB	390	0.017	2800	1	1	1	228.6	90	8.3
73	150	280	37.6	540	0	0	2.5	CFRP	U	390	0.008	3000	0.334	25	190	300	90	10.8
74	150	280	37.6	540	0	0	3	CFRP	U	390	0.008	3000	0.334	25	95	300	90	31.5
75	150	120	49.5	540	0	0	3	CFRP	U	390	0.008	3000	0.334	25	80	150	90	18.6
76	150	120	49.5	540	0	0	3	CFRP	U	390	0.008	3000	0.334	25	40	150	90	33.7
77	150	250	41.43	534	0.268	170	3.1	CFRP	U	230	0.015	3450	0.165	1	1	300	90	52.9
78	150	250	41.43	534	0.268	170	3.1	CFRP	U	231	0.015	3465	0.33	1	1	300	90	57.8
79	150	250	41.43	534	0.268	200	3.1	CFRP	U	230	0.015	3450	0.165	1	1	300	90	55.8
80	150	250	41.43	534	0.268	200	3.1	CFRP	U	230	0.015	3450	0.33	1	1	300	90	60.5
81	150	250	41.43	534	0.268	170	3.1	CFRP	U	230	0.015	3450	0.165	1	1	300	90	49.1
82	150	250	41.43	534	0.268	170	3.1	CFRP	U	230	0.015	3450	0.33	1	1	300	90	20.8
83	150	250	41.43	534	0.268	200	3.1	CFRP	U	230	0.015	3450	0.165	1	1	300	90	31.7
84	150	250	41.43	534	0.268	200	3.1	CFRP	U	230	0.015	3450	0.33	1	1	300	90	4

Table A1. *Cont.*

No	b	d	f_c	f_y	A_{sv}	S_v	a/d	FRP Type	Scheme	Ef	εfrp	ffrp	n^*t_f	wf	sf	hf	beta	Vexp
85	150	250	46.21	534	0.268	140	3.1	CFRP	U	230	0.015	3450	0.165	1	1	300	90	24.4
86	150	250	46.21	534	0.268	140	3.1	CFRP	U	230	0.015	3450	0.33	1	1	300	90	36.3
87	150	250	46.21	534	0.268	170	3.1	CFRP	U	230	0.015	3450	0.165	1	1	300	90	11.7
88	150	250	46.21	534	0.268	170	3.1	CFRP	U	230	0.015	3450	0.33	1	1	300	90	16.1
89	150	250	27.5	548	0	0	3	CFRP	SB	233.6	0.019	3350	0.165	1	1	300	90	45.3
90	150	250	27.5	548	0	0	3	CFRP	SB	233.6	0.019	3350	1.485	1	1	300	90	38.1
91	150	250	27.5	548	0	0	3	CFRP	SB	233.6	0.019	3350	1.485	1	1	300	90	65.5
92	150	250	31.4	548	0.268	200	3	CFRP	SB	233.6	0.019	3350	0.66	1	1	300	90	31.5
93	150	250	31.4	548	0.268	200	3	CFRP	SB	233.6	0.019	3350	1.485	1	1	300	90	51.8
94	150	250	31.4	548	0.268	200	3	CFRP	SB	233.6	0.019	3350	1.485	1	1	300	90	86
95	150	250	31.4	548	0.268	200	3	CFRP	SB	233.6	0.019	3350	0.66	1	1	300	90	47.3
96	150	250	31.4	548	0.268	200	3	CFRP	SB	233.6	0.019	3350	0.66	1	1	300	90	50.5
97	75	155	27.4	500	0.216	120	2.9	CFRP	U	23.5	0.016	4200	0.11	20	60	180	90	24.3
98	75	155	27.4	500	0.216	120	2.9	CFRP	U	23.5	0.016	4200	0.11	20	60	180	90	5.1
99	75	155	27.4	500	0.216	120	2.9	CFRP	F	23.5	0.016	4200	0.11	20	60	180	90	25.4
100	75	155	27.4	500	0.216	120	2.9	CFRP	F	23.5	0.016	4200	0.11	20	60	180	90	25.9
101	150	305	27.4	500	0.123	135	2.95	CFRP	U	23.5	0.016	4200	0.22	40	120	360	90	4.8
102	150	305	27.4	500	0.123	135	2.95	CFRP	U	23.5	0.016	4200	0.22	40	120	360	90	9.9
103	150	305	27.4	500	0.123	135	2.95	CFRP	F	23.5	0.016	4200	0.22	40	120	360	90	86.5
104	150	305	27.4	500	0.123	135	2.95	CFRP	F	23.5	0.016	4200	0.22	40	120	360	90	100.5
105	300	660	27.4	500	0.051	240	2.7	CFRP	U	23.5	0.016	4200	0.44	80	240	720	90	25.4
106	300	660	27.4	500	0.051	240	2.7	CFRP	U	23.5	0.016	4200	0.44	80	240	720	90	21.8
107	300	660	27.4	500	0.051	240	2.7	CFRP	F	23.5	0.016	4200	0.44	80	240	720	90	333.6
108	300	660	27.4	500	0.051	240	2.7	CFRP	F	23.5	0.016	4200	0.44	80	240	720	90	343.2
109	250	220	34.7	551	0	0	2.2	CFRP	SB	235	0.015	3550	0.2	1	1	250	90	91.5
110	250	220	34.7	552	0	0	2.2	CFRP	SB	235	0.015	3550	0.2	50	100	250	90	32
111	250	220	34.7	554	0	0	2.2	CFRP	SB	158	0.02	3160	0.2	1	1	250	90	45.5
112	250	220	34.7	555	0	0	2.2	CFRP	SB	230	0.02	3160	0.2	1	1	250	45	47.5
113	250	420	21	476	0.096	400	3	CFRP	F	392	0.007	2600	0.191	1	1	450	90	130
114	250	420	21	476	0.096	300	3	CFRP	F	392	0.007	2600	0.191	1	1	450	90	170
115	250	420	21	476	0.096	200	3	CFRP	F	392	0.007	2600	0.191	1	1	450	90	85
116	250	420	21	476	0.096	400	3	CFRP	U	392	0.007	2600	0.191	1	1	450	90	100
117	250	420	21	476	0.096	300	3	CFRP	U	392	0.007	2600	0.191	1	1	450	90	110
118	250	420	21	476	0.096	200	3	CFRP	U	392	0.007	2600	0.191	1	1	450	90	65
119	250	420	21	476	0.096	400	3	CFRP	SB	392	0.007	2600	0.191	1	1	450	90	55
120	250	420	21	476	0.096	300	3	CFRP	SB	392	0.007	2600	0.191	1	1	450	90	45
121	250	420	21	476	0.096	200	3	CFRP	SB	392	0.007	2600	0.191	1	1	450	90	25
122	250	420	21	476	0.096	400	4	CFRP	F	392	0.007	2600	0.191	1	1	450	90	80
123	250	420	21	476	0.096	400	4	CFRP	U	392	0.007	2600	0.191	1	1	450	90	60
124	250	420	21	476	0.096	400	4	CFRP	SB	392	0.007	2600	0.191	1	1	450	90	45
125	250	240	25.3	350	0.106	150	2.5	PET	F	10	0.074	740	0.14	1	1	270	90	13.8
126	250	240	25.3	350	0.106	150	2.5	PET	F	10	0.074	740	0.21	1	1	270	90	27.6
127	250	240	25.3	350	0.106	150	2.5	PET	F	10	0.074	740	0.28	1	1	270	90	26.4
128	250	240	25.3	350	0.106	150	2.5	PET	F	10	0.074	740	0.42	1	1	270	90	37.2
129	250	240	25.3	350	0.106	150	2.5	PET	F	10	0.074	740	0.56	1	1	270	90	60
130	250	450	32.6	350	0.056	150	2.5	PET	F	10	0.074	740	0.42	1	1	500	90	103.8
131	250	240	32.6	350	0.106	150	3.13	PET	F	10	0.074	740	0.21	1	1	270	90	77.4
132	250	240	32.6	350	0.106	150	2.5	PET	F	10	0.074	740	0.42	1	1	270	90	103.2
133	200	297	27.3	398	0.28	120	2	CFRP	U	270.5	0.005	3103	0.167	36	120	327	90	38.5
134	200	297	27.3	398	0.28	120	2	CFRP	U	270.5	0.008	3103	0.167	36	120	327	90	30.2
135	200	297	27.3	398	0.28	120	2	CFRP	U	270.5	0.01	3103	0.167	36	120	327	90	33.4
136	200	297	27.3	398	0.28	120	2	CFRP	U	270.5	0.007	3103	0.167	36	120	327	90	45.7
137	200	297	27.3	398	0.28	120	2	CFRP	U	270.5	0.005	3103	0.668	36	120	327	90	37.5
138	200	297	27.3	398	0.28	120	2	CFRP	U	270.5	0.006	3103	0.668	36	120	327	90	61.3
139	200	297	27.3	398	0.28	120	2	CFRP	U	270.5	0.007	3103	0.668	36	120	327	90	88
140	200	297	27.3	398	0.28	120	2	CFRP	U	270.5	0.012	3103	0.668	36	120	327	90	100.5
141	200	297	27.3	398	0.28	120	2	CFRP	U	270.5	0.007	3103	0.668	36	120	327	90	112.8
142	180	303	47	310	0.122	160	1	CFRP	U	235	0.004	4200	0.11	60	150	350	90	10
143	180	303	47	310	0.122	160	1.5	CFRP	U	235	0.008	4200	0.11	60	150	350	90	37
144	180	303	47	310	0.122	160	2	CFRP	U	235	0.008	4200	0.11	60	150	350	90	68
145	180	303	47	310	0.122	160	2.5	CFRP	U	235	0.008	4200	0.11	60	150	350	90	62
146	180	303	55	310	0.122	160	3	CFRP	U	235	0.007	4200	0.11	60	150	350	90	41

Table A1. *Cont.*

No	b	d	f_c	f_y	A_{sv}	S_v	a/d	FRP Type	Scheme	Ef	εfrp	ffrp	n^*t_f	wf	sf	hf	beta	Vexp
147	180	303	55	310	0.122	160	3.5	CFRP	U	235	0.007	4200	0.11	60	150	350	90	53
148	150	250	23.3	527	0.22	300	3	CFRP	U	390	0.008	3000	0.165	1	1	300	90	53.9
149	150	250	23.3	527	0.33	200	3	CFRP	U	390	0.008	3000	0.165	1	1	300	90	39.6
150	200	400	33.8	500	0.07	200	3.2	CFRP	U	230	0.015	3500	0.11	50	400	450	90	41.2
151	200	400	36	500	0.07	400	3.2	CFRP	U	230	0.015	3500	0.11	50	400	450	90	33.4
152	200	400	35.8	500	0.07	400	3.2	CFRP	U	230	0.015	3500	0.11	50	400	450	90	30.1
153	200	400	34.7	500	0.07	400	3.2	CFRP	F	230	0.015	3500	0.11	50	200	450	90	98.9
154	120	150	40	280	0.39	120	2.57	CFRP	SB	230	0.015	3500	0.26	50	100	260	90	20
155	120	150	40	280	0.39	120	2.57	CFRP	SB	230	0.015	3500	0.26	50	100	260	90	16.3
156	120	150	40	280	0.39	120	2.57	CFRP	SB	230	0.015	3500	0.26	50	100	260	90	13.8
157	120	175	40	280	0.39	120	2.57	CFRP	F	230	0.015	3500	0.26	50	100	200	90	25
158	120	175	40	280	0.39	120	2.57	CFRP	F	230	0.015	3500	0.26	50	100	200	90	23.8
159	120	175	40	280	0.39	120	2.57	CFRP	F	230	0.015	3500	0.26	50	100	200	90	22.5
160	150	210	16.9	498.2	0.16	200	2.4	BFRP	U	89	0.035	3115	0.14	75	50	260	90	25.2
181	150	300	50.35	494	0	0	2	CFRP	SB	234.5	0.02	3450	0.34	300	900	300	90	47.15
182	150	300	51.38	494	0	0	2	CFRP	SB	234.5	0.02	3450	0.34	150	600	150	90	8.75
183	150	300	49.38	494	0	0	2	CFRP	SB	234.5	0.02	3450	0.34	75	900	300	90	3.9
184	150	300	48.41	494	0	0	2	CFRP	SB	234.5	0.02	3450	0.34	150	900	150	90	8.75
185	250	360	36.95	500	0.11	380	3.5	CFRP	U	63	0.011	700	1	300	200	150	90	138.3
186	250	360	36.95	500	0.11	380	3.5	CFRP	U	63	0.011	700	1	300	200	150	90	91.5
187	250	360	24.47	500	0.11	380	3.5	CFRP	U	63	0.011	700	1	1	1	150	90	96.26
188	250	360	24.47	500	0.11	380	3.5	CFRP	U	63	0.011	700	1	1	1	150	90	55.37
189	250	360	22.64	500	0.11	380	3.5	CFRP	U	63	0.011	700	1	1	1	150	90	133.6
190	250	360	22.64	500	0.11	380	3.5	CFRP	U	63	0.011	700	1	1	1	150	90	136.6
191	250	360	20.5	500	0.11	380	3.5	CFRP	U	63	0.011	700	1	300	200	150	90	123
192	250	360	20.5	500	0.11	380	3.5	CFRP	U	63	0.011	700	1	300	200	150	90	142.9
193	200	173	29.3	665.3	0.163	160	3	CFRP	U	230	0.015	3430	0.165	1	1	210	90	19.3
194	203	305	25.2	420	0	0	3	CFRP	U	228	0.015	3450	0.165	76	229	368	90	46.7
195	305	457	32	420	0	0	3	CFRP	U	228	0.015	3450	0.165	152	305	546	90	87.2
196	406	610	32	420	0	0	3	CFRP	U	228	0.015	3450	0.165	252	381	698.5	90	126.8

References

1. Çiftçioğlu, A.Ö.; Naser, M.Z. Hiding in plain sight: What can interpretable unsupervised machine learning and clustering analysis tell us about the fire behavior of reinforced concrete columns? *Structures* **2022**, *40*, 920–935. [CrossRef]
2. Shafaei, H.; Naderpour, H. Seismic fragility evaluation of FRP-retrofitted RC frames subjected to mainshock-aftershock records. *Structures* **2020**, *27*, 950–961. [CrossRef]
3. Hemmatian, A.; Jalali, M.; Naderpour, H.; Nehdi, M.L. Machine learning prediction of fiber pull-out and bond-slip in fiber-reinforced cementitious composites. *J. Build. Eng.* **2023**, *63*, 105474. [CrossRef]
4. De Maio, U.; Gaetano, D.; Greco, F.; Lonetti, P.; Pranno, A. The damage effect on the dynamic characteristics of FRP-strengthened reinforced concrete structures. *Compos. Struct.* **2023**, *309*, 116731. [CrossRef]
5. Nwankwo, C.O.; Mahachi, J.; Olukanni, D.O.; Musonda, I. Natural fibres and biopolymers in FRP composites for strengthening concrete structures: A mixed review. *Constr. Build. Mater.* **2023**, *363*, 129661. [CrossRef]
6. Zhou, X.-Y.; Qian, S.-Y.; Wang, N.-W.; Xiong, W.; Wu, W.-Q. A review on stochastic multiscale analysis for FRP composite structures. *Compos. Struct.* **2022**, *284*, 115132. [CrossRef]
7. Zhang, F.; Gao, L.; Wu, Y.-F.; Liu, J. Flexural design of reinforced concrete structures strengthened with hybrid bonded FRP. *Compos. Struct.* **2021**, *269*, 113996. [CrossRef]
8. Pohoryles, D.A.; Melo, J.; Rossetto, T.; Varum, H.; D'Ayala, D. Effect of slab and transverse beam on the FRP retrofit effectiveness for existing reinforced concrete structures under seismic loading. *Eng. Struct.* **2021**, *234*, 111991. [CrossRef]
9. Wei, X.; Russell, J.; Živanović, S.; Mottram, J.T. Measured dynamic properties for FRP footbridges and their critical comparison against structures made of conventional construction materials. *Compos. Struct.* **2019**, *223*, 110956. [CrossRef]
10. Ferracuti, B.; Savoia, M.; Zucconi, M. RC frame structures retrofitted by FRP-wrapping: A model for columns under axial loading and cyclic bending. *Eng. Struct.* **2020**, *207*, 110243. [CrossRef]
11. Markou, G.; Garcia, R.; Mourlas, C.; Guadagnini, M.; Pilakoutas, K.; Papadrakakis, M. A new damage factor for seismic assessment of deficient bare and FRP-retrofitted RC structures. *Eng. Struct.* **2021**, *248*, 113152. [CrossRef]
12. Ding, Z.; Li, L.; Wang, X.; Yu, T.; Xia, Y. Vibration-based FRP debonding detection using a Q-learning evolutionary algorithm. *Eng. Struct.* **2023**, *275*, 115254. [CrossRef]
13. Zeng, J.J.; Chen, S.P.; Feng, P.; Zhuge, Y.; Peng, K.D.; Dai, J.G.; Fan, T.H. FRP bar-reinforced ultra-high-performance concrete plates with a grouting sleeve connection: Development and flexural behavior. *Eng. Struct.* **2023**, *287*, 116164. [CrossRef]
14. Wu, R.; Xu, R.; Wang, G. Modeling and prediction of short/long term mechanical behavior of FRP-strengthened slabs using innovative composite finite elements. *Eng. Struct.* **2023**, *281*, 115727. [CrossRef]

15. Khalilpourazari, S.; Doulabi, H.H. A flexible robust model for blood supply chain network design problem. *Ann. Oper. Res.* **2022**, *328*, 701–726. [CrossRef]
16. Khalilpourazari, S.; Teimoori, S.; Mirzazadeh, A.; Pasandideh, S.H.R.; Tehrani, N.G. Robust Fuzzy chance constraint programming for multi-item EOQ model with random disruption and partial backordering under uncertainty. *J. Ind. Prod. Eng.* **2019**, *36*, 276–285. [CrossRef]
17. Tirkolaee, E.B.; Goli, A.; Weber, G.-W. Fuzzy Mathematical Programming and Self-Adaptive Artificial Fish Swarm Algorithm for Just-in-Time Energy-Aware Flow Shop Scheduling Problem With Outsourcing Option. *IEEE Trans. Fuzzy Syst.* **2020**, *28*, 2772–2783. [CrossRef]
18. Chen, T.; Guestrin, C. XGBoost: A Scalable Tree Boosting System. In Proceedings of the 22nd ACM SIGKDD International Conference on Knowledge Discovery and Data Mining, San Francisco, CA, USA, 13–17 August 2016; Association for Computing Machinery: New York, NY, USA, 2016; pp. 785–794.
19. Breiman, L. Random Forests. *Mach. Learn.* **2001**, *45*, 5–32. [CrossRef]
20. Freund, Y.; Schapire, R.E. Experiments with a New Boosting Algorithm. In Proceedings of the 13th International Conference on International Conference on Machine Learning, Bari, Italy, 3–6 July 1996.
21. Wu, X.; Kumar, V.; Ross Quinlan, J.; Ghosh, J.; Yang, Q.; Motoda, H.; McLachlan, G.J.; Ng, A.; Liu, B.; Yu, P.S.; et al. Top 10 Algorithms in Data Mining. *Knowl. Inf. Syst.* **2008**, *14*, 1–37. [CrossRef]
22. Zou, H.; Hastie, T. Regularization and Variable Selection via the Elastic Net. *J. R. Stat. Soc. Ser. B Stat. Methodol.* **2005**, *67*, 301–320. [CrossRef]
23. Fix, E.; Hodges, J.L. Discriminatory Analysis. Nonparametric Discrimination: Consistency Properties. *Int. Stat. Rev./Rev. Int. Stat.* **1989**, *57*, 238–247. [CrossRef]
24. Zhang, Y.; Haghani, A. A Gradient Boosting Method to Improve Travel Time Prediction. *Transp. Res. Part C Emerg. Technol.* **2015**, *58*, 308–324. [CrossRef]
25. Naser, M.Z. Observational Analysis of Fire-Induced Spalling of Concrete through Ensemble Machine Learning and Surrogate Modeling. *J. Mater. Civ. Eng.* **2021**, *33*, 04020428. [CrossRef]
26. Monti, G.; Liotta, M. Tests and design equations for FRP-strengthening in shear. *Constr. Build. Mater.* **2007**, *21*, 799–809. [CrossRef]
27. Khalifa, A.; Nanni, A. Rehabilitation of rectangular simply supported RC beams with shear deficiencies using CFRP composites. *Constr. Build. Mater.* **2002**, *16*, 135–146. [CrossRef]
28. Pellegrino, C.; Modena, C. An experimentally based analytical model for the shear capacity of FRP-strengthened reinforced concrete beams. *Mech. Compos. Mater.* **2008**, *44*, 231–244. [CrossRef]
29. Adhikary, B.; Mutsuyoshi, H. Behavior of Concrete Beams Strengthened in Shear with Carbon-Fiber Sheets. *J. Compos. Constr. J Compos. Constr.* **2004**, *8*, 258–264. [CrossRef]
30. Diagana, C.; Li, A.; Gedalia, B.; Delmas, Y. Shear strengthening effectiveness with CFF strips. *Eng. Struct.* **2003**, *25*, 507–516. [CrossRef]
31. Ianniruberto, U.; Imbimbo, M. Role of fiber reinforced plastic sheets in shear response of reinforced concrete beams: Experimental and analytical results. *J. Compos. Constr.* **2004**, *8*, 415–424. [CrossRef]
32. Cao, S.Y.; Chen, J.F.; Teng, J.G.; Hao, Z.; Chen, J. Debonding in RC beams shear strengthened with complete FRP wraps. *J. Compos. Constr.* **2005**, *9*, 417–428. [CrossRef]
33. Carolin, A.; Täljsten, B. Theoretical study of strengthening for increased shear bearing capacity. *J. Compos. Constr.* **2005**, *9*, 497–506. [CrossRef]
34. Zhang, Z.; Hsu, C.-T.T. Shear strengthening of reinforced concrete beams using carbon-fiber- reinforced polymer laminates. *J. Compos. Constr.* **2005**, *9*, 158–169. [CrossRef]
35. Barros, J.A.O.; Dias, S.J.E. Near surface mounted CFRP laminates for shear strengthening of concrete beams. *Cem. Concr. Compos.* **2006**, *28*, 276–292. [CrossRef]
36. Pellegrino, C.; Modena, C. Fiber-reinforced polymer shear strengthening of reinforced concrete beams: Experimental study and analytical modeling. *ACI Struct. J.* **2006**, *103*, 720–728.
37. Pellegrino, C.; Modena, C. Fiber reinforced polymer shear strengthening of reinforced concrete beams with transverse steel reinforcement. *J. Compos. Constr.* **2002**, *6*, 104–111. [CrossRef]
38. Leung, C.K.Y.; Chen, Z.; Lee, S.; Ng, M.; Xu, M.; Tang, J. Effect of size on the failure of geometrically similar concrete beams strengthened in shear with FRP strips. *J. Compos. Constr.* **2007**, *11*, 487–496. [CrossRef]
39. Kim, G.; Sim, J.; Oh, H. Shear strength of strengthened RC beams with FRPs in shear. *Constr. Build. Mater.* **2008**, *22*, 1261–1270. [CrossRef]
40. Grande, E.; Imbimbo, M.; Rasulo, A. Experimental Response of RC Beams Strengthened in Shear by FRP Sheets. *Open Civ. Eng. J.* **2015**, *7*, 127–135. [CrossRef]
41. Tidarut, J.; Jian-Guo, D.; Dawei, Z.; Mineo, S.; Tamon, U. Experimental Study on Shear Behavior of Reinforced-Concrete Members Fully Wrapped with Large Rupture-Strain FRP Composites. *J. Compos. Constr.* **2014**, *18*, A4013009. [CrossRef]
42. Hu, Z.; Zhou, X.; Guo, M.; Huang, X.; Hu, B. Enhancing the Performance of CFRP Shear-Strengthened RC Beams Using 'Ductile' Anchoring Devices. *Front. Mater.* **2020**, *7*, 292. [CrossRef]
43. Li, W.; Leung, C.K.Y. Effect of shear span-depth ratio on mechanical performance of RC beams strengthened in shear with U-wrapping FRP strips. *Compos. Struct.* **2017**, *177*, 141–157. [CrossRef]

44. Gonzalez-Libreros, J.H.; Sneed, L.H.; D'Antino, T.; Pellegrino, C. Behavior of RC beams strengthened in shear with FRP and FRCM composites. *Eng. Struct.* **2017**, *150*, 830–842. [CrossRef]
45. Matthys, S. *Structural Behaviour and Design of Concrete Members Strengthened with Externally Bonded FRP Reinforcement*; Ghent University: Ghent, Belgium, 2000.
46. Tan, Z.; Ye, L.P. Experimental research on shear capacity of RC beam strengthened with externally bonded FRP sheets. *China Civ. Eng. J.* **2003**, *36*, 12–18.
47. Allam, S.; Ebeido, T. Retrofitting of RC beams predamaged in shear using CFRP sheets. *Alex. Eng. J.* **2003**, *42*, 87–101.
48. Saribiyik, A.; Abodan, B.; Balci, M.T. Experimental study on shear strengthening of RC beams with basalt FRP strips using different wrapping methods. *Eng. Sci. Technol. Int. J.* **2021**, *24*, 192–204. [CrossRef]
49. Bukhari, I.A.; Vollum, R.L.; Ahmad, S.; Sagaseta, J. Shear strengthening of reinforced concrete beams with CFRP. *Mag. Concr. Res.* **2010**, *62*, 65–77. [CrossRef]
50. Bukhari, I.A.; Vollum, R.; Ahmad, S.; Sagaseta, J. Shear Strengthening of Short Span Reinforced Concrete Beams with CFRP Sheets. *Arab. J. Sci. Eng.* **2013**, *38*, 523–536. [CrossRef]
51. Alzate, A.; Arteaga, Á.; de Diego, A.; Perera, R. Shear strengthening of reinforced concrete beams using fibre reinforced polymers (frp). *Eur. J. Environ. Civ. Eng.* **2009**, *13*, 1051–1060. [CrossRef]
52. Rizzo, A.; De Lorenzis, L. Behavior and capacity of RC beams strengthened in shear with NSM FRP reinforcement. *Constr. Build. Mater.* **2009**, *23*, 1555–1567. [CrossRef]
53. Bae, S.; Tann, B.; Belarbi, A. Size effect of reinforced concrete beams strengthened in shear with externally bonded CFRP sheets. In Proceedings of the 6th International Conference on FRP Composites in Civil Engineering (CICE 2012), Rome, Italy, 13–15 June 2012.
54. Zaitseva, E.; Rabcan, J.; Levashenko, V.; Kvassay, M. Importance analysis of decision making factors based on fuzzy decision trees. *Appl. Soft Comput.* **2023**, *134*, 109988. [CrossRef]

Disclaimer/Publisher's Note: The statements, opinions and data contained in all publications are solely those of the individual author(s) and contributor(s) and not of MDPI and/or the editor(s). MDPI and/or the editor(s) disclaim responsibility for any injury to people or property resulting from any ideas, methods, instructions or products referred to in the content.